
Masters Theses

Student Theses and Dissertations

Spring 2022

Zinc plating from alkaline non-cyanide bath

Abdul J. Mohammed

Follow this and additional works at: https://scholarsmine.mst.edu/masters_theses



Part of the [Metallurgy Commons](#)

Department:

Recommended Citation

Mohammed, Abdul J., "Zinc plating from alkaline non-cyanide bath" (2022). *Masters Theses*. 8091.
https://scholarsmine.mst.edu/masters_theses/8091

This thesis is brought to you by Scholars' Mine, a service of the Missouri S&T Library and Learning Resources. This work is protected by U. S. Copyright Law. Unauthorized use including reproduction for redistribution requires the permission of the copyright holder. For more information, please contact scholarsmine@mst.edu.

ZINC PLATING FROM ALKALINE NON-CYANIDE BATH

by

ABDUL JALIL MOHAMMED

A THESIS

Presented to the Graduate Faculty of the

MISSOURI UNIVERSITY OF SCIENCE AND TECHNOLOGY

In Partial Fulfillment of the Requirements for the Degree

MASTER OF SCIENCE

in

METALLURGICAL ENGINEERING

2022

Approved by:

Michael Moats, Advisor
Wayne Huebner
Lana Alagha

© 2022

Abdul Jalil Mohammed

All Rights Reserved

PUBLICATION THESIS OPTION

This thesis consists of the following two articles, formatted in the style used by the Missouri University of Science and Technology:

Paper I, found on pages 18-39, has been published as Mohammed, A.J. & Moats, M (2022). Effects of Carrier, Leveller, and Booster Concentrations on Zinc Plating from Alkaline Zincate Baths. *Metals*, 12, 621. <https://doi.org/10.3390/met12040621>.

Paper II, found on pages 40-60, is intended for submission to the 2023 TMS Conference Proceedings for publication.

ABSTRACT

Alkaline non-cyanide zinc plating baths are preferred when trying to avoid the toxicity of cyanide baths or corrosivity of acid baths. Without additives, alkaline zincate baths produce powdery non-adherent deposits which have no use in commercial plating. Additives must be added at optimum concentrations to produce adherent, bright and uniform zinc deposits. In this study electrochemical tests were used to determine effects of additives on cathodic polarization, throwing power and morphology of deposits. Current density distribution in a unique bath of 37.5 g L^{-1} Zn and 210 g L^{-1} NaOH was modelled using COMSOL and validated two plating cells with different geometries.

ACKNOWLEDGMENTS

Foremost, I am grateful to my parents and brothers for educating and preparing me for my future.

I would like to express my sincere gratitude to my research supervisor, Dr. Michael Moats for the opportunity, guidance, and advice throughout my study period. I would like to say a big thank you to Dr. Arezoo Emdadi and Dr. Yijia Gu for their help in modelling my experimental setups.

My completion of this research could not have been accomplished without the support of my friends and colleagues, Florian, Joe, Weston, Jamie, Bailey, Asebi and Richard. Special thanks to Kareem Mukhtar and Dr. Charles Abbey, God bless you for encouraging me to pursue a graduate degree.

I also want to thank the staff of the Materials Science and Engineering Department: Teneke, Emily, Brian, and Nathan for all the support and assistance.

Finally, to my caring, loving, and supportive wife, Tradece, thank you for your patience.

TABLE OF CONTENTS

	Page
PUBLICATION THESIS OPTION.....	iii
ABSTRACT.....	iv
ACKNOWLEDGMENTS	v
LIST OF ILLUSTRATIONS.....	ix
LIST OF TABLES	xi
 SECTION	
1. INTRODUCTION.....	1
2. LITERATURE REVIEW.....	3
2.1. PRE-TREATMENTS	3
2.1.1. Alkaline cleaning.....	4
2.1.2. Electrolytic Cleaning.....	6
2.1.3. Acid Pickling.....	6
2.2. ELECTROGALVANIZING.....	7
2.2.1. Cyanide Zinc Bath.....	7
2.2.2. Acid Zinc Bath	9
2.2.3. Alkaline Non-Cyanide Bath (Zincate)	10
2.2.4. Additives	12
2.3. POST-PLATE TREATMENT.....	15
2.3.1. Nitric dip.....	15
2.3.2. Chromating.....	15

2.4. EFFLUENT TREATMENT AND DISPOSAL	16
PAPER	
I. EFFECTS OF CARRIER, LEVELLER AND BOOSTER CONCENTRATIONS ON ZINC PLATING FROM ALKALINE ZINCATE BATHS	18
ABSTRACT	18
1. INTRODUCTION	19
2. EXPERIMENTAL	22
2.1. HULL CELL STUDIES	23
2.2. ZINC COATING CHARACTERIZATION.....	24
2.3. ELECTROCHEMICAL EXPERIMENTS	24
2.4. CURRENT EFFICIENCY (CE) AND THROWING POWER (TP)	25
3. RESULTS AND DISCUSSION	25
3.1. DEPOSIT APPEARANCE AND BRIGHTNESS	25
3.2. DEPOSIT MORPHOLOGY.....	29
3.3. ELECTROCHEMICAL STUDIES	30
3.4. THROWING POWER AND CATHODIC CURRENT EFFICIENCY	33
4. CONCLUSIONS	35
REFERENCES	36
II. SIMULATION OF CURRENT DENSITY DISTRIBUTION IN ELECTROGALVANIZATION CELL	40
ABSTRACT	40
1. INTRODUCTION	41
2. EXPERIMENTAL	45
2.1. PLATING BATH	45

2.2. CATHODIC POLARIZATION	45
2.3. ROTATING CYLINDER HULL CELL	46
2.4. LABORATORY TUBE PLATING CELLS	47
3. COMPUTATIONAL MODELLING OF ALKALINE ZINCATE ELECTROGALVANIZING.....	50
3.1. ROTATING CYLINDER HULL CELL (RCHC) MODELLING.....	51
3.2. LABORATORY TUBE PLATING CELL	52
4. RESULTS AND DISCUSSION	53
4.1. FUNDAMENTAL ELECTROCHEMICAL DATA	53
4.2. RCHC SIMULATION AND EXPERIMENTAL RESULTS	53
4.3. LABORATORY TUBE PLATING CELL SIMULATION AND RESULTS.	55
5. CONCLUSIONS	58
REFERENCES.....	59
SECTION	
3. CONCLUSIONS AND RECOMMENDATIONS.....	61
3.1. CONCLUSIONS	61
3.2. RECOMMENDATIONS.....	62
BIBLIOGRAPHY.....	63
VITA.....	70

LIST OF ILLUSTRATIONS

PAPER I	Page
Figure 1. Hull cell deposit appearance produced from 1, 2, 3 and 4 % additive concentrations.....	26
Figure 2. Hull cell deposit appearance produced by plating baths with various additive concentrations (see Table 1).....	27
Figure 3. a) Pareto chart of absolute and b) Normal probability plot of the standardized effects of additives on gloss as determined by ANOVA with significant set at $\alpha < 0.05$	30
Figure 4. SEM images of Hull cell deposits at a current density of 305 A m^{-2} . Labels correspond to baths I to IX in Table 1.....	31
Figure 5. Cathodic polarization of plating baths with 37.5 g L^{-1} zinc and 210 g L^{-1} NaOH at $40 \text{ }^\circ\text{C}$ produced at a sweep rate of 1 mV s^{-1}	33
Figure 6. (a)Pareto chart and b) Normal probability plot of the standardized effects of additives on throwing power.	35
PAPER II	
Figure 1. A schematic diagram of a s standard Hull cell used to evaluate electroplating coating thickness and appearance [11].	42
Figure 2. A 2-D schematic cross-section of a rotating cylinder Hull cell (RCHC) showing the anode (counter electrode), the cathode (working electrode) on a rotating shaft and an electrical insulator.....	44
Figure 3. Laboratory tube plating cell.....	48
Figure 4. Schematic drawing of the laboratory setup; (a) top view of the tank, and (b) the conductor rail.....	49
Figure 5. (a) The geometry of RCHC and (b) the finite element mesh distribution for the 2D axisymmetric RCHC model.....	51
Figure 6. (a) The schematic cross-section of the lab-setup plating cell, (b) the mesh size and distribution used in the finite element modeling.	53
Figure 7. Cathode current density (i) vs overpotential ($E-E_0$). The blue dots are the lab measurement data..	54

Figure 8. The experimental measurements (error bars are +/- 2 standard deviation) and the computational calculation of cathode current density for RCHC, and (b) a schematic of each section position along the cathode.....	55
Figure 9. The stream distribution of the electrolyte potential.....	56
Figure 10. Computational results for the distribution of the current density along the simulated tube for 6 different positions on the conducted rail and an average of the values.	56
Figure 11. Computational and experimental results for the distribution of the current density along the tube.....	57
Figure 12. Tube plated from custom built laboratory plating cell. Points 1, 2 and 3 shows the rail marks due to contact to the cathode during the electrogalvanization process.	58

LIST OF TABLES

SECTION	Page
Table 2.1. Types of soils encountered in electrogalvanization [5].	4
Table 2.2. Composition of cyanide zinc baths (g L^{-1}) [16].	8
Table 2.3. Fluoborate and sulfate electroplating bath compositions..	9
Table 2.4. Composition and operating characteristics of acid chloride zinc plating baths for rack and barrel processing cycles.....	10
Table 2.5. Composition of Typical Alkaline Zincate Baths [2].	12
 PAPER I	
Table 1. Additive concentrations of baths used in this study.	23
Table 2. Average gloss values of Hull cell deposits produced between 215 to 325 Am^{-2}	28
Table 3. Throwing power and cathodic current efficiency for the plating baths with additive concentrations provided in Table 1 with a current density of 305 A m^{-2} at the anode in the Haring Blum Cell (throwing power) and cathode in two-electrode cell (current efficiency)..	34
 PAPER II	
Table 1. The RCHC operation parameters values and descriptions.	52

1. INTRODUCTION

Steel's ability to withstand both thermal and physical stress has made it the preferred choice in the construction and manufacturing of a wide variety of structures. Exposure of steel to oxygen and moisture causes it to corrode (oxidize). For this reason, steel is coated with a less corrosive metal, paint, or enamel to provide corrosion protection. Zinc provides excellent protection to steel due to its relatively slow corrosion rate over a wide range of conditions.

Zinc corrodes slowly because it forms a natural protection barrier. Zinc reacts with oxygen to form a thin layer of zinc oxide which combines with water to form zinc hydroxide. Zinc hydroxide in turn reacts with carbon dioxide from the air producing zinc carbonate. Zinc carbonate is a thin stable layer which protects the underlying zinc resulting in low corrosion rate of the coating (7 to 8 times slower than that of iron) in most environments [1].

Another mechanism by which zinc protects the underlying steel is through galvanic protection. Zinc has a more negative standard reduction potential than iron. Therefore, zinc will oxidize prior to iron if both are exposed to the environment (e.g., zinc coating is scratched) and there is an electrolyte between them (e.g., a water droplet covers the scratch). This mechanism is referred to as cathodic protection. Through cathodic protection, the zinc coating can protect the steel even when a portion of the steel is exposed due to damage to the zinc coating [2]. Because of zinc's protection capabilities, approximately half of the world's 13 million tonnes of refined zinc is used to coat or galvanize steel [1].

The primary reason for coating a steel substrate is to protect it from exposure to adverse conditions. The coating process must be able to produce a protective layer that is impervious and adheres properly to the surface of the steel. The most common galvanization methods are hot-dip galvanization, electrogalvanization, zinc-rich painting, zinc spraying, mechanical plating and sherardizing [1, 3]. The most used industrial methods are hot-dip galvanization and electrogalvanization. Continual technological improvements make it difficult to conclude in favor of one process over the other. However, hot dip always includes some surface alloying by diffusion, and the deposit thickness is less easily controlled than in electroplating [4]. Electrogalvanization is done at a relatively lower temperature therefore does not affect the mechanical property of the steel substrate. It also produces uniform, bright, and adhering coating to the steel.

This research aims to determine the effects and possible interactions of three commercial additives (Eldiem carrier, Eldiem booster and Bright Enhancer 2x) on zinc electrodeposition from a high concentration alkaline non-cyanide bath.

The second part of the study was to develop an electroplating model to simulate the current density distribution along the cathode in a high concentration alkaline non-cyanide bath. COMSOL Multiphysics software was used in the development of the model, and it was tested for validity using two cells of different geometry.

2. LITERATURE REVIEW

Electro galvanization comprises of three main processes, namely: pretreatment, electroplating and post-plate treatment. These processes complement each other; therefore, each must be performed properly to attain a quality product.

2.1. PRE-TREATMENTS

Electro galvanization is a surface process, therefore the nature of the surface to be plated influences the nature of the coating. For this reason, surface preparation of substrate is very important prior to the electroplating process. Most metals are soiled by metal processes such as casting, machining, welding, labelling and preservation. These processes introduce various surface soils.

Unlike cyanide zinc baths which have inherent cleaning abilities and therefore can tolerate poorly cleaned substrates, alkaline non-cyanide and acid zinc baths produce poor deposits when substrate surfaces are not thoroughly cleaned. Surface contaminations prevent proper adhesion of the zinc to the electroplated surface. The soil type and chemical properties of the substrate are to be taken into consideration when selecting a pretreatment method and cleaning agent. The cleaning method and agent should be able to efficiently remove the soil without damaging the surface of the substrate. Table 2.1 summarizes different types of soils and how they can be removed by either alkaline cleaning or acid pickling. Thus, both pre-treatment steps are commonly used in sequence and are equally important to obtain a good surface prior to electroplating. The substrate is

rinsed after each step to prevent contamination of subsequent baths due to drag-out of solution.

Table 2.1. Types of soils encountered in electrogalvanization [5].

Soil removed by alkaline cleaning	Soil removed by acid pickling
Pigmented drawing compounds	Heat treatment scale
Unpigmented drawing compounds	Rust
Rustproofing oils	Oxide films
Grease	Tarnish films
Buffing compounds	Smuts
Quenching oils	Welding scale
Fingerprints	
Polishing compounds	

2.1.1. Alkaline Cleaning. Alkaline cleaning is the first stage of the pre-treatment process where oils, grease, wax, and dirt are removed from the steel surface. Most zinc plating plants use proprietary alkaline cleaners for their operations. A good alkaline cleaner should not attack the metal surface or produce fumes and must be free rinsing. Alkaline cleaning is performed at high temperature (65 to 95°C) [5] to ensure efficient removal of oil and grease adhering to the metal surface. Alkaline cleaners contain emulsifiers, soaps and/or wetting agents that enhances the penetrating power of the organic solvent and permits removal of the stains and associated soil by power flushing [6].

Alkaline cleaners are divided into light and heavy-duty cleaners. Light duty cleaners are typically run at temperature ranging from 66 °C to boiling and at concentration between 4 to 8 g L⁻¹ NaOH. Heavy duty cleaners on the other hand operate at higher concentrations (80 to 240 g L⁻¹ NaOH) and a temperature range of 60 to 70 °C [7].

The mechanism of alkaline cleaning in the removal of soil is by a combination of the following principles:

Saponification – Sodium hydroxide converts the fats and oils contained in the soils to form water-soluble soaps [8]. The soap formed from the saponification process enhances the cleaning efficiency.

Surfactants – Surface active or wetting agents in the cleaner reduce the surface tension at the metal-soil interface resulting in the lifting of the soil from the metal surface [9].

Dispersion and Emulsification – An emulsification is a dispersion of one liquid in another liquid of which both are obviously immiscible [10]. Surfactants in cleaners and soap formed by saponification emulsifies the oily soils into tiny droplets which then disperse in the cleaning solution until rinsing is complete.

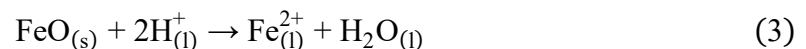
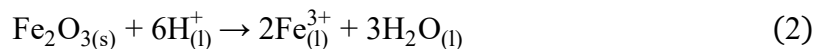
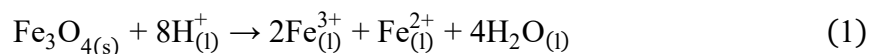
Metallic ions such as calcium, magnesium or manganese hinder the efficiency of a cleaner by using up the surfactants. Sequestration and chelation are when agents in the cleaners complex with metallic ions to form stable soluble complexes. This allows the surfactants in the cleaner to function efficiently [11]. Complex sodium phosphates and sodium gluconates are used as sequestering and chelation agents, respectively. Use of polyphosphate-type sequestering agents is limited to temperatures below 80 °C because

decomposition into orthophosphates occurs above this temperature. Organic chelating agents are stable to above 100°C [6].

The correct formulation of alkaline cleaner should be that which can efficiently get rid of the soil for subsequent process after rinsing.

2.1.2. Electrolytic Cleaning. After alkaline cleaning, the steel can be subjected to electrolytic cleaning. This process removes more strongly adhered soils that escaped alkaline cleaning and removes or loosens metallic oxide for acid pickling. The metal surface is submitted to electrolysis by dipping it into a conducting solution and connected to an external power source [12]. Cleaning can be carried out both cathodically and anodically. In most operations the metal is made the anode to enhance vigorous cleaning by oxygen gas evolution. Anodic cleaning eliminates the deposition of metallic smuts on the substrate but may lead to hydrogen embrittlement of the substrate [5].

2.1.3. Acid Pickling. Acid pickling is usually the last pretreatment step prior to electrogalvanizing. The main purposes of pickling are the removal of tenuous scales, oxides, and rust and to activate the steel surface for electroplating. Pickling is carried out by dipping the steel in strong acid for an optimum period. The typical temperature range for pickling is between 30 to 40°C with an acid concentration of 8 to 50% volume acid based on the type of acid being utilized [5]. Hydrochloric and sulfuric acid are commonly used in the zinc plating industry. The mechanism of acid pickling is shown by the Reactions 1-4 [13]:





Reactions 1-3 illustrate the dissolution of iron oxides from the steel surface.

Reaction 4 indicates that it is possible to dissolve the substrate if pickling takes too long. Therefore, the pickling duration should be long enough to dissolve scale or oxide without dissolving the metal. Inhibitors are sometimes added to prevent the dissolution of the metal surface during acid pickling. Due to issues caused by some inhibitors in the electroplating process, most zinc plating operations try to avoid their usage.

The pickled surface is rinsed with deionized water after acid pickling before transferred to the electrogalvanization process tank. The rinsing is carried out to prevent drag-out from acid pickling bath to the electrogalvanization stage. The rinsing process also serves as a surface cleanliness evaluation. A well cleaned surface does not form water droplets or beads when it comes in contact with water. There are other sophisticated surface cleanliness evaluation techniques such as, as radio isotope, UV fluorescence, conductivity method, surface potential difference, electrochemical measurements, and optical stimulated electron emission among others [7]. The "water break free" surface evaluation is widely used because it is practical and gives an acceptable evaluation.

2.2. ELECTROGALVANIZING

The three most common bath in electrogalvanization are cyanide bath, acid bath and alkaline non-cyanide bath (Zincate).

2.2.1. Cyanide Zinc Bath. Cyanide baths dominated the electrogalvanization industry for many years due to the flexibility of operation and its tolerance to impurities.

Relatively minimum operating requirements are needed to produce acceptable zinc coating.

Despite the performance and operator friendly nature of cyanide zinc baths, there has been a shift away from its use due to health and environmental hazards as well as the high cost of effluent treatment [14]. Efforts were made to reduce the cyanide concentration without impairing the characteristics of the deposit. Additives were formulated which produced bright deposits over a wide current range, at sodium cyanide concentrations as low as 7.5 g L^{-1} [15]. This led to the development of mid, low, and micro cyanide baths which had relatively lower cyanide concentrations compared to the regular cyanide baths as shown in Table 2.2.

In an effort to produce a cyanide free plating bath, the alkaline noncyanide and bright acid zinc baths were developed.

Table 2.2. Composition of cyanide zinc baths (g L^{-1}) [16].

Constituent	Regular	Mid	Low	Micro
Zn(CN)_2	60	30	10	7.5
NaCN	40	20	8	1
NaOH	80	75	65	75
NaCO_3	15	15	15	-
Na_xS_y	2	2	-	-
Brightener	1-4	1-4	1-4	1-5

2.2.2. Acid Zinc Bath. In 1852, acid zinc electrolytes became the first bath to be patented for zinc electrodeposition [17] but its continuous use in the 20th century was hindered due to dull deposits, poor covering and throwing power and development of bright cyanide baths [16]. Work on acid sulphate bath by Saubestre et al. [18] and subsequent development of bright acid zinc processes revolutionized bright acid zinc plating [19]. Between 45-50% of zinc electroplating operations in developed nations is from acid zinc baths [20]. Acid baths are preferred for their high cathode efficiency and quick brightening action which provide faster plating rate hence increased productivity [21]. However, acid bath comes with problems of corrosivity and poor throwing power. Acid plating baths can be categorized into acid sulfate [22, 23] and acid chloride [24, 25] baths based on the constituents as shown in Tables 2.3 and 2.4. Sodium chloride can be used to substitute a part of either ammonium or potassium chloride to produce a mixed acid bath [26]

Table 2.3. Fluoborate and sulfate electroplating bath compositions. (a) At room temperature; 3.5 to 4 pH; at 1076 to 6458 A m⁻². (b) At 30 to 52 °C; 3 to 4 pH; at 1076 to 6458 A m⁻². (c) As required [27].

Constituent	Fluoborate ^(a) g L ⁻¹	Sulfate ^(b) g L ⁻¹
Zinc	65-105	135
Zinc fluoborate	225-375	-
Zinc sulfate	-	375
Ammonium fluoborate	30-45	-
Ammonium chloride		7.5-22.5
Addition agent	(c)	(c)

Table 2.4. Composition and operating characteristics of acid chloride zinc plating baths for rack and barrel processing cycles. (a)Carrier and primary brighteners for acid chloride are proprietary, and exact recommendations of manufacturer should be followed. Values given are representative [27].

Constituent	Ammoniated bath (Barrel)		Ammoniated bath (Rack)	
	Optimum	Range	Optimum	Range
Preparation				
Zinc chloride	18 g L ⁻¹	15-25 g L ⁻¹	30 g L ⁻¹	19-56 g L ⁻¹
Ammonium chloride	120 g L ⁻¹	100-150 g L ⁻¹	180 g L ⁻¹	120-200 g L ⁻¹
Potassium chloride	-	-	-	-
Sodium chloride	-	-	-	-
Boric Acid	-	-	-	-
Carrier brightener ^(a)	4%	3-5 %	3-5 %	3-4 %
Primary brightener ^(a)	0.25%	0.1-0.3 %	0.25%	0.1-0.3 %
pH	5.6	5.5-5.8	5.8	5.2-6.2
	Potassium bath		Mixed sodium ammonium bath (barrel)	
	Optimum	Range	Optimum	Range
Zinc chloride	71 g L ⁻¹	62-85 g L ⁻¹	34 g L ⁻¹	31-40 g L ⁻¹
Ammonium chloride	-	-	30 g L ⁻¹	25-35 g L ⁻¹
Potassium chloride	207 g L ⁻¹	186-255 g L ⁻¹	-	-
Sodium chloride	-	-	120 g L ⁻¹	100-140 g L ⁻¹
Boric Acid	34 g L ⁻¹	30-380 g L ⁻¹	-	-
Carrier brightener ^(a)	4%	4-5 %	4%	3-5 %
Primary brightener ^(a)	0.25%	0.1-0.3 %	0.20%	0.1-0.3 %
pH	5.2	4.8-5.8	5	4.8-5.3

2.2.3. Alkaline Non-Cyanide Bath (Zincate). Alkaline zincate baths solve the problems of toxicity of cyanide-based baths and corrosion of acid baths but they have their own shortcomings. Alkaline zincate baths tend to form powdery non-adherent deposits without the use of additives [28]. Although zincate baths have good throwing power, they form microporous coating, and this has been attributed to the evolution of

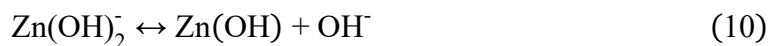
hydrogen at the cathode. Complexing agents are sometimes used to inhibit hydrogen evolution [29].

There have been several proposed mechanisms to explain the deposition of zinc in alkaline zincate baths. The first, proposed by Benner [30] is shown in Reactions 5-7:

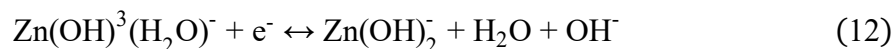


The discharged species in Benner's proposed mechanism is Zn(OH)_2 which gains two electrons in Reaction 6 to form Zn(OH)^{2-} which loses OH^- to become Zn.

A four step mechanism proposed by Bockris et al. [31] and referred to in subsequent literature is described in Reactions 8-11:



The discharged species in this mechanism is Zn(OH)_3^- and the rate determining step is Reaction 9. Since Zn^{2+} prefers to exist as a tetra or hexa-coordinate species, $\text{Zn(OH)}_3^-(\text{H}_2\text{O})^-$, Reaction 9 can be replaced by (12):



The rate of reaction 12 is still generally faster than the rate of transport of electroactive species to the site of discharge, resulting in powdery non-adherent deposits. In order to achieve bright and useful deposits, the rate of Reaction 12 must be minimized

[32]. Organic additives are therefore added to either modify Reaction 12 or enhance selective deposition.

An alkaline zincate solution consists in its simplest form as zinc metal dissolved into a concentrated sodium hydroxide solution. The composition of an electrolyte plays an important role in the efficiency of the bath. Sodium hydroxide improves conductivity in the electrolyte and zinc anode dissolution. The concentration of these compositions differs from operation to operation. Generally, there are two classification of composition ranges as shown in Table 2.5.

Table 2.5. Composition of Typical Alkaline Zincate Baths [2].

Composition	Low chemistry	High Chemistry
Zinc	6-9 g L ⁻¹	13.5-22.5 g L ⁻¹
Sodium hydroxide	75-105 g L ⁻¹	120-150 g L ⁻¹
Additives	1-3 %	1-3 %

Alkaline noncyanide zincate baths have relative narrow operating range for zinc concentration, for this reason the single most critical factor in the operation of a zincate bath is the zinc concentration [5, 33]. Therefore, it is very important to keep the zinc concentration as close as possible to the optimum zinc metal content.

2.2.4. Additives. Alkaline noncyanide baths were considered as able to give only dark, spongy or powdery deposits over normal plating current densities and it was necessary to replace the complexing effect of cyanide ions by other complexing agents like EDTA, gluconate, tartrate and triethanolamine [5]. However, this caused a new

effluent problem due to complexing effect of chelating agents which resulted in problems in heavy metal removal in effluent treatment. Modern alkaline zincate baths additives are often organic compounds that when added to the plating bath in small amounts can modify the crystal growth, thus changing the properties of the deposits [34]. The use of synthetic quaternary ammonium compounds (QACs) as additives permitted the development of modern alkaline free-cyanide zinc electrolytes [14].

Additives can be classified into carriers, brighteners and levellers [35]. The carrier enables grain refinement by polarizing the zinc surface which increases the energy available to speed up the transport of Zn atoms into the growing Zn lattice [36]. Typical carriers used in alkaline zincate baths are polyvinyl alcohol (PVA) [37], tetra ethylene pent amine (TEPA) [38] and sodium potassium tartrate [39]. Brighteners on the other hand aid in attaining bright deposits, most brighteners are made of aldehyde group compounds such as piperonal (PIP), anisaldehyde and veratraldehyde (VER) [40]. Brighteners are small organic molecules with aldehyde, ketone, and sulfur containing functional groups [41].

There have been many studies on the effect of additives in alkaline zincate bath. Yuan et al. [42] studied the electrochemical behavior and mechanism of quaternary ammonium salt and sulfonated salt of nicotinic acid additives. They found that increasing the amount of quaternary ammonium salt additive increased the nucleation overpotential. The rate determining step of zinc electrodeposition in the presence of quaternary ammonium salt additive is changed from mixed control step to electrochemical control step. The sulfonated salt of nicotinic acid had little effect on the nucleation overpotential. Addition of quaternary aliphatic polyamine (QAA) to an alkaline zincate bath resulted in

decrease in exchange current density, smaller grain size and change in crystal structure [43]. Polyvinyl alcohol which is the most commonly used carrier ensures uniform thickness distribution and refined grain in alkaline zincate baths [37]. Other studies on additives has been on combinations of anthranillic acid (ANA) and furfural (FFL) [2], DL-alanine (DLA) and glutaraldehyde [44] and polyamine and quaternized pyridine carboxylic acid [45].

Another additive classification is levellers which are used to promote the deposition on sites with low current density, such as cavities [34]. Levelers adsorb onto high points during deposition to promote deposition in recesses which tends to result in a more uniform coating thickness [34]. Levelling mechanism research works related to copper and nickel is mostly used to describe the effects of levelers in zinc deposition due to lacking literature in zinc. Moreover the mechanism of levelling in copper and nickel are applicable to electroplating of zinc [46]. One of these theories is the diffusional theory of levelling in a paper by Kardos [47]. The diffusional theory states that the adsorption of the organic compound on the electrode surface inhibits the metal deposition reaction simply by exerting a “blocking” effect, that is, the electrode reaction cannot occur on the sites occupied by the organic molecule. If adsorption kinetics of the organic molecule is controlled by diffusion, due to variation in the diffusion layer thickness over the microprofile, a greater number of adsorptions will be on the micropeaks due to smaller diffusion layer thickness compared to the microrecesses. Therefore available deposition sites will be at the microrecess site [48].

Additives are also widely used in acid zinc baths to produce acceptable deposits. Many studies such as the use of polyethylene glycol (PEG) [24] and syringaldehyde

(SGA) to produce nanocrystalline bright zinc deposits from acid chloride baths can be found in literature [41]. The mixture of PEG and SGA improved the morphology and orientation of zinc platelets. The prospect of using thiourea derivatives as additives to inhibit the zinc dendrite formation in ammonium chloride electrolyte was also studied by Yang et al. [49]. Addition of small amounts of tartaric acid to zinc sulfate bath has been found to produce smooth semi-bright deposit with finer grains [50].

The specific chemical compounds used as additives in large industrial alkaline zinc plating facilities are proprietary.

2.3. POST-PLATE TREATMENT

Plated parts undergo post-plate treatment to improve the durability and appearance of the coating. Commonly used post-plate treatments are nitric dip and chromating.

2.3.1. Nitric Dip. Zinc plated parts are thoroughly rinsed with water right after the electroplating process to prevent staining by dragged out electrolyte and then thoroughly dried to prevent water stains. Parts plated from zincate and cyanide baths have a yellowish appearance and are dipped into a weak nitric acid (0.25 to 1% vol.) to smoothen the zinc surface and give it a bright a color. This process is called bright dip or nitric strike. Black spots on plated parts after nitric strike is an indication of metallic contamination in the zinc bath [5]. Parts are rinsed after the nitric strike and sent for chromating.

2.3.2. Chromating. The final step is a secondary coating to provide extra corrosion protection to the zinc coating. Chromate films which were first patented by E.J

Wilhelm in 1936 [51] are the most used post-plate coating. Hexavalent chromium gives the best corrosion protection, but the toxicity of Cr (VI) has caused a shift towards the use of trivalent chromium which is less toxic. Chromate films come in varying colors of blue, yellow, olive, or black [52]. Other post-plate coatings are molybdate, cerate and permanganate-based coatings [53]. However, chromating has the advantage of variability of colors, ease of application, adhesion, and low cost [54].

2.4. EFFLUENT TREATMENT AND DISPOSAL

Electro galvanization operations can discharge copious amounts of effluents containing heavy metals. Electroplating baths are rarely disposed when properly maintained and treated for contaminants periodically. For this reason, effluents are mostly from rinse tanks due to contamination from drag out of electrolyte by electroplated components. Zinc concentration from electroplating rinse water vary between 0.112 to 252 mg L⁻¹ [55, 56]. Rinse effluents may contain cyanide, zinc, acids, chlorides, and grease that pose environmental and health hazard if not treated before release into the environment. Zinc and zinc compounds are included in the list of toxic pollutants by the United States Environmental Protection agency [57]. Discharge of electroplating wastewater into surface water not only causes environmental pollution, but also adversely affects aquatic and human life. Moreover, the concentration of zinc in effluents is above the pollution norms. The United States Environmental Protection Agency set standard zinc effluent concentration for electroplating plants at 4.2 mg L⁻¹ daily maximum and 2.6 mg L⁻¹ maximum for a four day average [58].

Electro galvanization effluents are treated in multiple steps due to the nature of the various contaminants. Oil and greases in wastewater which float on the surface are skimmed off and incinerated. The cyanide in the wastewater is then treated by multiple cyanide destructive process. The next step which is zinc removal can be carried out by methods such as chemical precipitation [59], adsorption [60], ion exchange [61], solvent extraction [62] and electrocoagulation [63]. Treated wastewater can either be discharged into the environment or reused by the plating facility.

PAPER**I. EFFECTS OF CARRIER, LEVELLER AND BOOSTER CONCENTRATIONS ON ZINC PLATING FROM ALKALINE ZINCATE BATHS**

Abdul Jalil Mohammed and Michael Moats*

Materials Research Center
Missouri University of Science and Technology
Rolla, MO, USA 65409

*Corresponding author, moatsm@mst.edu

ABSTRACT

Organic additives are required for alkaline zincate plating baths to obtain an acceptable coating on steel for corrosion protection. The effects and possible interactions of three commercial additives (Eldiem carrier, Eldiem booster and Bright enhancer 2x) on zinc electrodeposition from a high concentration alkaline zincate bath were investigated. Visually acceptable deposits were produced within the current density range of 130 to 430 A m⁻² for most additive conditions examined. Over concentration ranges examined, decreasing the booster concentration led to brighter zinc deposits and an interaction between the carrier and booster was detected. The additives fostered the formation of compact and adherent coatings as illustrated by scanning electron microscopy. Throwing power and current efficiency were not impacted by the additives over the concentration ranges examined. Linear sweep voltammetry proved the additives increased the overpotential for zinc deposition. The additive combination that produced

the brightest deposit also demonstrated the strongest adsorption of additives in linear sweep voltammetry.

1. INTRODUCTION

Steel's strength, ductility and low cost has made it a preferred choice in the construction and manufacturing of a wide variety of structures. A major disadvantage of steel is that it corrodes when exposed to oxygen and moisture. To overcome this disadvantage, steel is coated with a less corrosive metal, paint or enamel to provide corrosion protection. Zinc provides excellent protection to steel due to its relatively slow corrosion rate over a wide range of conditions [1].

The most common industrial methods for zinc coating of steel are hot-dip galvanizing and electrogalvanizing. Continual technological improvements make it difficult to conclude in favor of one process over the other. However, hot-dip always includes some surface alloying by diffusion, and the deposit thickness is less easily controlled than in electrogalvanizing [2]. Electrogalvanizing is performed at a lower temperature than hot-dipping and does not affect the mechanical property of the steel substrate. It can also produce a uniform, bright and adhering coating to the steel. Electrogalvanizing is often preferred over hot-dipping when a decorative finish is desired [3].

Cyanide based zinc baths dominated the electrogalvanizing industry for many years due to their efficiency and ease of utilization, but their use has gradually declined over time due to the toxicity of cyanide and increasingly stringent environmental

regulations [4, 5]. For these reasons, there has been a shift towards the use of less toxic acid zinc and alkaline zincate (non-cyanide) baths.

Alkaline zincate baths solve the problems of toxicity of cyanide-based baths and the inherent corrosivity of acid baths on equipment while exhibiting a reasonable throwing power [6, 7]. However, the absence of the complexing effect of cyanide results in the production of powdery non-adherent deposits from alkaline zincate baths [8]. To produce smooth and adherent zinc coating, plating additives are required in alkaline zincate baths.

The most common plating additives are classified as carriers, levellers, and brighteners [9]. Classifications are based on the properties of additives (like chemical nature) and their impact on the zinc electrodeposit, such as grain refiner and smoothing agent [9]. Positively charged additives can assist the negatively charged zincate ion approach and absorb onto the negatively charged cathode [10]. For alkaline zincate baths, carriers such as polyvinyl alcohol [11, 12], polypropylene imine and sodium potassium tartrate [13] polarize the cathode which results in grain refinement. While carriers refine the grains, they do not necessarily produce a bright finish [14]; therefore, brighteners are used to complement the effect of the carrier to produce a bright deposit [15]. Polyamines [16, 17] and aldehyde [18] are widely used as brightening agents in alkaline zincate baths. Levelers adsorb onto high points during deposition to promote deposition in recesses which tends to result in a more uniform coating thickness [17]. Condensation products like amines and aldehydes have been used to produce additives that have both brightening and leveling capabilities [19]. Additives are known to have synergistic effects on microstructure and appearance of zinc coatings [20, 21]. The specific chemical

compounds used as additives in large industrial alkaline zinc plating facilities are proprietary.

The zinc and sodium hydroxide concentrations of alkaline zincate baths also have profound effects on the nature of the deposit. Typical concentration ranges are 6 to 22 g L⁻¹ zinc and 60 to 150 g L⁻¹ NaOH [8]. According to Wantotayan et al. [22], Zn and NaOH concentrations affect the coating thickness and throwing power. Sodium hydroxide also influences the conductivity of the bath and current efficiency. Nayaka and Venkatesha [19] studied the effect of Zn and NaOH on the current density range which produced acceptable deposits and determined that increasing the Zn and NaOH content widened the operating window.

Scott and Moats [23] studied the effects of low concentrations of three commercial additives: Eldiem Carrier, Eldiem Booster and Bright Enhancer 2x (leveler) in an unusually high Zn (37.5 g L⁻¹) and NaOH (210 g L⁻¹) bath relative to other literature sources. The study revealed that improvements to the zinc deposit appearance could be made, but none of the conditions examined produced a desirable bright and shiny deposits. Therefore, in this study the same commercial additives and bath chemistry were used but at higher additive concentrations. Both the individual and synergistic effects of these commercial additives on deposit brightness, cathodic polarization, throwing power, current efficiency and surface morphology were investigated.

2. EXPERIMENTAL

Plating baths or electrolytes were prepared by dissolving high purity zinc balls (Belmont Metals) into a NaOH solution. Analytical reagent grade NaOH (Fisher Chemicals) and deionized and distilled water (18.3 M Ω .cm) were used to prepare the solution. The solution was then treated with Special High Grade (SHG) zinc dust (Purity Zinc Metals) at a concentration of 3 g L⁻¹. After mixing the dust with the solution for 120 minutes at room temperature, the solution was filtered using Whatman grade 1 qualitative filter paper to remove any residual solids. Electrolysis using a mild steel anode and stainless-steel cathode was then performed with the filtrate at a current density of 10 A m⁻² for 5 hours to further rid the solution of metal contaminants. The zinc and sodium hydroxide concentrations were determined by titration and then diluted to 37.5 g L⁻¹ zinc and 210 g L⁻¹ NaOH using de-ionized water.

Three commercial additives - Eldiem Carrier, Eldiem Booster and Bright Enhancer 2x (leveler) – were used in this study without further purification. The plating additives were added to the electrolyte and preheated for 60 minutes prior to each experiment. All experiments were performed at 40°C (\pm 2°C).

A target ratio of 5:2:1 for carrier, leveller and booster, respectively, was indicated by Scott as producing the best zinc finish at low total additive concentration (~0.07%) [24]. Preliminary Hull cell experiments were performed using the 5:2:1 additive ratio with total additive concentrations at 1, 2, 3 and 4%, which are more typical of commercial levels for other additive systems [8]. From these results, 1% (bath I) additives concentration with a ratio of 5:2:1 was selected as the center point for a 2³ full

factorial design of experiments to examine the individual effects of these additives along with possible interactions [25] on Hull cell plating appearance, deposit structure, throwing power, current efficiency, and electrochemical response. Low and high values were selected at -50% and +50% of the midpoint concentrations producing the design of experiments shown in Table 1.

2.1. HULL CELL STUDIES

A 267 mL Lucite Hull cell (Kocour) was used with a mild steel mesh anode. The cathode was a zinc coated 1010 steel panel of dimension 10 cm x 7.6 cm. Prior to each experiment the cathode was dipped in 50% v/v HCl to strip off the zinc coating and then rinsed with DI water until a water break-free surface was observed. A current of 2 A was applied using a Extech (Model 382275) for 5 minutes without external electrolyte agitation. After plating, the cathode was rinsed with deionized water, dipped in 0.5% nitric acid for 10 seconds and then rinsed again with deionized water. The rinsed sample was air dried to avoid water stains on the zinc coating.

Table 1. Additive concentrations of baths used in this study.

Bath	Carrier (mL/L)	Leveler (mL/L)	Booster (mL/L)
I	6.25	2.50	1.25
II	9.38	3.75	0.63
III	3.13	3.75	0.63
IV	9.38	3.75	1.88
V	9.38	1.25	1.88
VI	3.13	1.25	1.88
VII	9.38	1.25	0.63
VIII	3.13	1.25	0.63
IX	3.13	3.75	1.88

2.2. ZINC COATING CHARACTERIZATION

The surface morphology of the Hull cell deposits at the 320 A m^{-2} location was examined using a TESCAN-ASCAT scanning electron microscopy operated at 20 kV.

Deposit (215 to 325 A m^{-2} range on Hull cell cathode) brightness was measured using a BYK micro-TRI-gloss glossmeter at a measurement angle of 85° . Specular reflection occurs at the surfaces of reflecting objects, and this is attributed to glossiness [26].

2.3. ELECTROCHEMICAL EXPERIMENTS

Electrochemical tests were performed in a three-electrode cell. A rotating 316L stainless-steel working electrode disc (5mm diameter), platinum mesh counter electrode and mercury/mercury sulfate (MSE) reference electrode were used. The reference electrode was placed in a Luggin tube filled with the test solution. The tip of the Luggin tube was 1.5 cm from the surface of the working electrode. The working electrode was rotated at 500 rpm to minimize mass transport limitations. The solution was sparged with nitrogen gas for 10 minutes to remove oxygen before each experiment. The working electrode was pre-plated with zinc for 5 minutes using a current density of 320 A m^{-2} . Then linear sweep voltammetry (LSV) was employed by scanning the working electrode potential from -1.9 to -2.2 V vs. MSE at a scan rate of 1 mV/s. The electro-chemical tests were performed using a Gamry 3000 potentiostat.

2.4. CURRENT EFFICIENCY (CE) AND THROWING POWER (TP)

A rectangular cell (7.2 x 15 cm) with a 1010 steel panel as the cathode and a mild steel mesh as the anode was used to measure current efficiency (CE). Zinc was electrodeposited for 15 minutes at a cathode current density of 305 A m⁻². The cathodes were weighed before and after the experiment to obtain the mass of the deposit. The theoretical mass (m) was calculated using Faraday's law, Equation 1:

$$m = \frac{ItM}{nF} \quad (1)$$

where I was the current applied (A) in time t (s), n is number of electrons involved in the reaction, M is the molar mass of zinc and F is Faraday's constant (96485 C/mol). The percentage of the measured mass to the theoretical mass is CE.

A Haring-Blum cell [27] was used for the throwing power experiments. Throwing power (% TP) was calculated using Field's formula [3], Equation 2:

$$\%TP = \frac{L - M}{L + M - 2} \times 100 \quad (2)$$

where L is the ratio of the distance between the further and the nearer cathode (5:1) and M is the ratio of the mass of deposit on the nearer to further cathode.

3. RESULTS AND DISCUSSION

3.1. DEPOSIT APPEARANCE AND BRIGHTNESS

Preliminary Hull cell experiments were used to center our design of experiments. Plating baths with 1%, 2%, 3% and 4% additives concentrations at a ratio of 5:2;1 (carrier: booster: leveler) [24] were examined. The visual appearance of the zinc deposits

produced in these experiments are shown schematically in Figure 1. The 1% additive bath produced the widest range of current density with a bright appearance. Thus, 1% additives concentration was used as the center point for the 2^3 full factorial design of experiments to evaluate individual effects and interactions.

To observe the magnitude of the individual and synergistic effects of the additives on the zinc coating appearance and structure, Hull cell experiments were conducted with the additive concentrations shown in Table 1. The visual appearances of the Hull cell deposits are summarized in Figure 2.

Deposits were characterized as burnt, white, streaky, bright, mirror bright and gray. No mirror bright deposits were produced in all the baths under the current density range observed in this study.

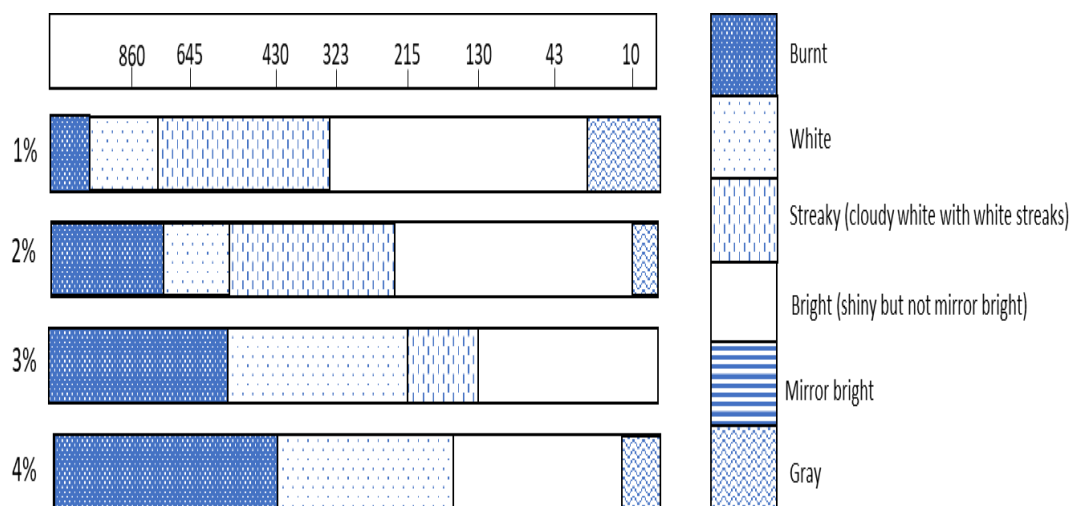


Figure 1. Hull cell deposit appearance produced from 1, 2, 3 and 4 % additive concentrations. Bath composition was 37.5 g L^{-1} zinc and 210 g L^{-1} NaOH held at $40 \text{ }^\circ\text{C}$. A Hull cell ruler is presented at the top with current densities in A m^{-2} .

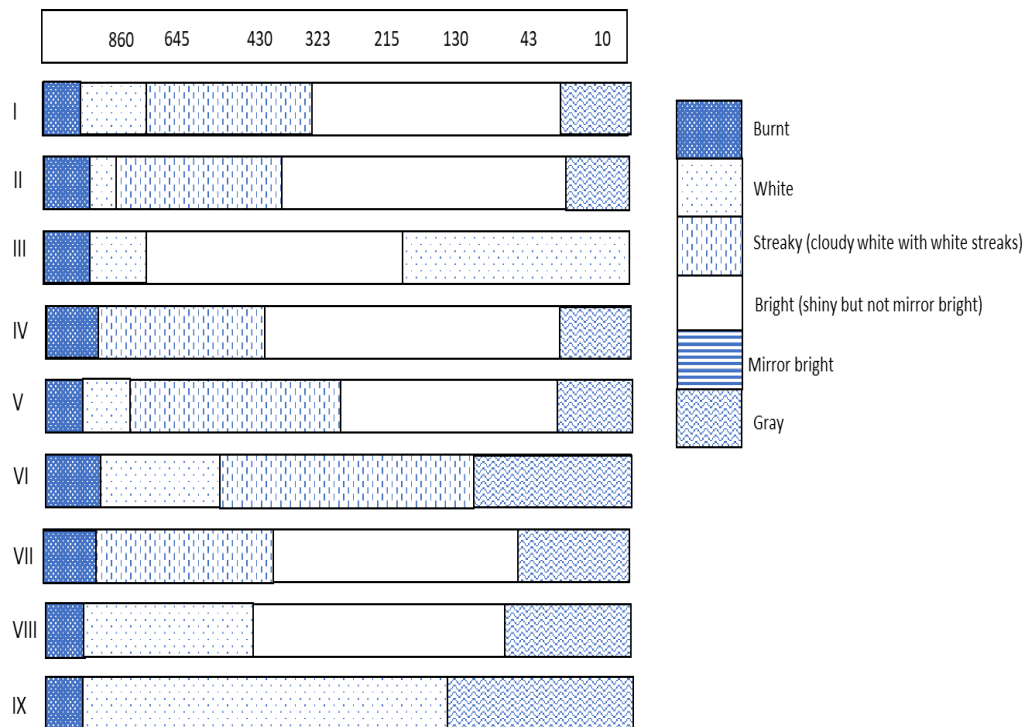


Figure 2. Hull cell deposit appearance produced by plating baths with various additive concentrations (see Table 1). Bath composition was 37.5 g L⁻¹ zinc and 210 g L⁻¹ NaOH held at 40 °C. A Hull cell ruler is presented at the top with current densities in A m⁻².

As seen in Figure 2, current densities above 960 A m⁻² resulted in burnt (or black) deposits for all baths while gray deposits were observed at the low current density end except for bath III which had a white streaky appearance at low current densities. Most of the baths produced bright deposits between ~50 and 325 A m⁻² except baths III, VI and IX. A bright deposit was produced by bath III from 215 to 750 Am⁻². Baths VI and IX did not produce a bright deposit at any current density.

The average glossiness (brightness) of deposits in the current density range from 215 to 325 A m⁻² are reported in Table 2. This range was selected to represent industrially relevant conditions. Baths III and VI produced the brightest and least bright deposits, respectively.

Table 2. Average gloss values of Hull cell deposits produced between 215 to 325 A m⁻².

Bath	Gloss
I	71
II	70
III	85
IV	70
V	62
VI	35
VII	75
VIII	80
IX	55

An analysis of variance (ANOVA) was performed using MINITAB software for a 2³ factorial design with a center point with the gloss value as the output response. The magnitudes of individual and synergistic effects of the additives were determined and the ANOVA results are summarized in Figure 3. The standardized effects are tests of the null hypothesis that the effect is 0. The reference line indicates which effects are statistically significant at a significance level denoted by alpha ($\alpha=0.005$). Over the concentration ranges examined, booster concentration and the interaction between booster and carrier had a statistically significant effect on brightness as their standardized effects were greater than 4.303. Individually, carrier and leveller concentrations were not determined to be statistically significant on brightness.

The normal probability plot (shown in Figure 3b) shows the standardized effects relative to a distribution fit line for the case when all the effects are zero. The booster concentration shows a negative effect hence decreasing booster concentration enhanced brightness. The interaction between carrier and booster had a positive impact and resulted in greater brightness. Primary additives or carriers are typically added at higher concentrations compared to secondary additives or brighteners (booster). The carrier may serve as a hydrotrope to increase the solubility of the booster [28]. Therefore, increasing carrier concentration with the proper amount of booster tended to enhance brightness. Proper carrier concentration ensures the brightener (booster) is solubilized and stabilized [29].

3.2. DEPOSIT MORPHOLOGY

Figure 4 shows the surface morphology of deposits obtained from baths I to IX at 305 A m⁻². Nodules or bumps were observed on the surface of coatings produced from baths VI and IX which resulted in a rougher deposit with low gloss values. Deposits produced from the remaining baths exhibited circular depressions on their surfaces. These depressions are believed to be caused by hydrogen gas formation. The simultaneous evolution of hydrogen and reduction of zinc at the cathode resulted in depressions due to gas bubbles remaining on the zinc deposit. The growth of rougher zinc within the depressions are observed in several images in Figure 4. It is proposed that hydrogen evolution can lead to desorption of adsorbed additives which in turn promotes the deposition of rougher zinc at those locations.

Bath III had the least number of bumps and hydrogen evolution sites, which is believed to have caused the highest gloss value measured in this study. The synergistic effects of the additives generally helped to produce compact and dense deposit in the baths.

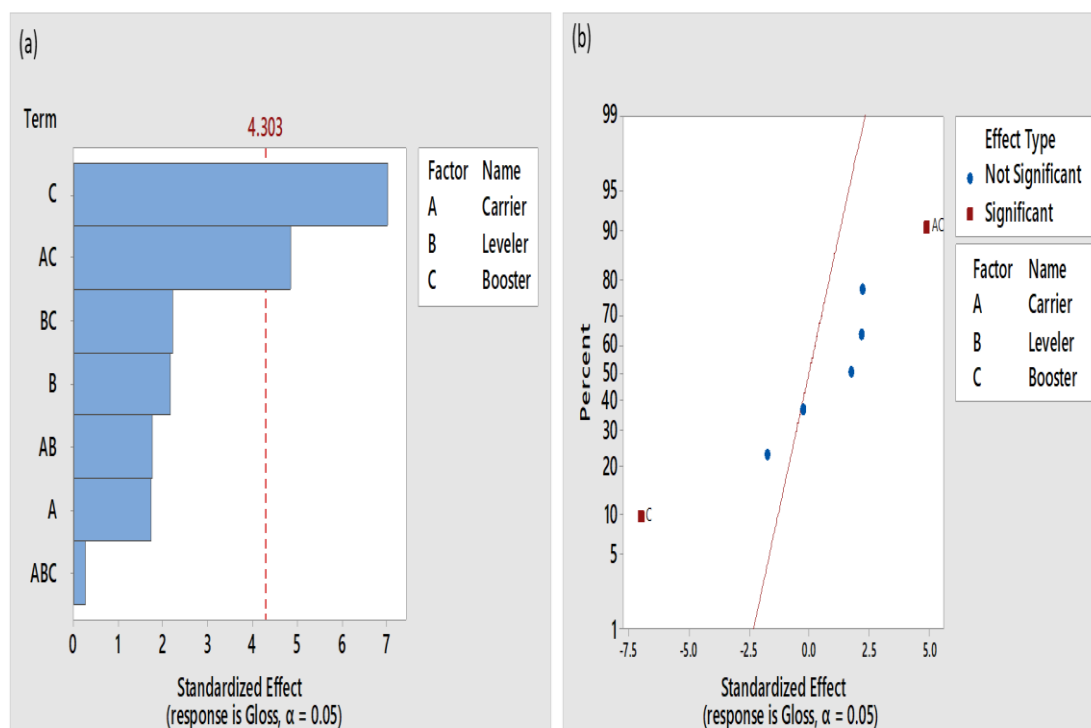


Figure 3. a) Pareto chart of absolute values and b) Normal probability plot of the standardized effects of additives on gloss as determined by ANOVA with significant set at $\alpha < 0.05$.

3.3. ELECTROCHEMICAL STUDIES

Cathodic polarization studies were carried out to understand the effect of the additives on the zinc reduction process. Figure 5 illustrate the linear sweep voltammograms generated for each bath including a bath without additives.

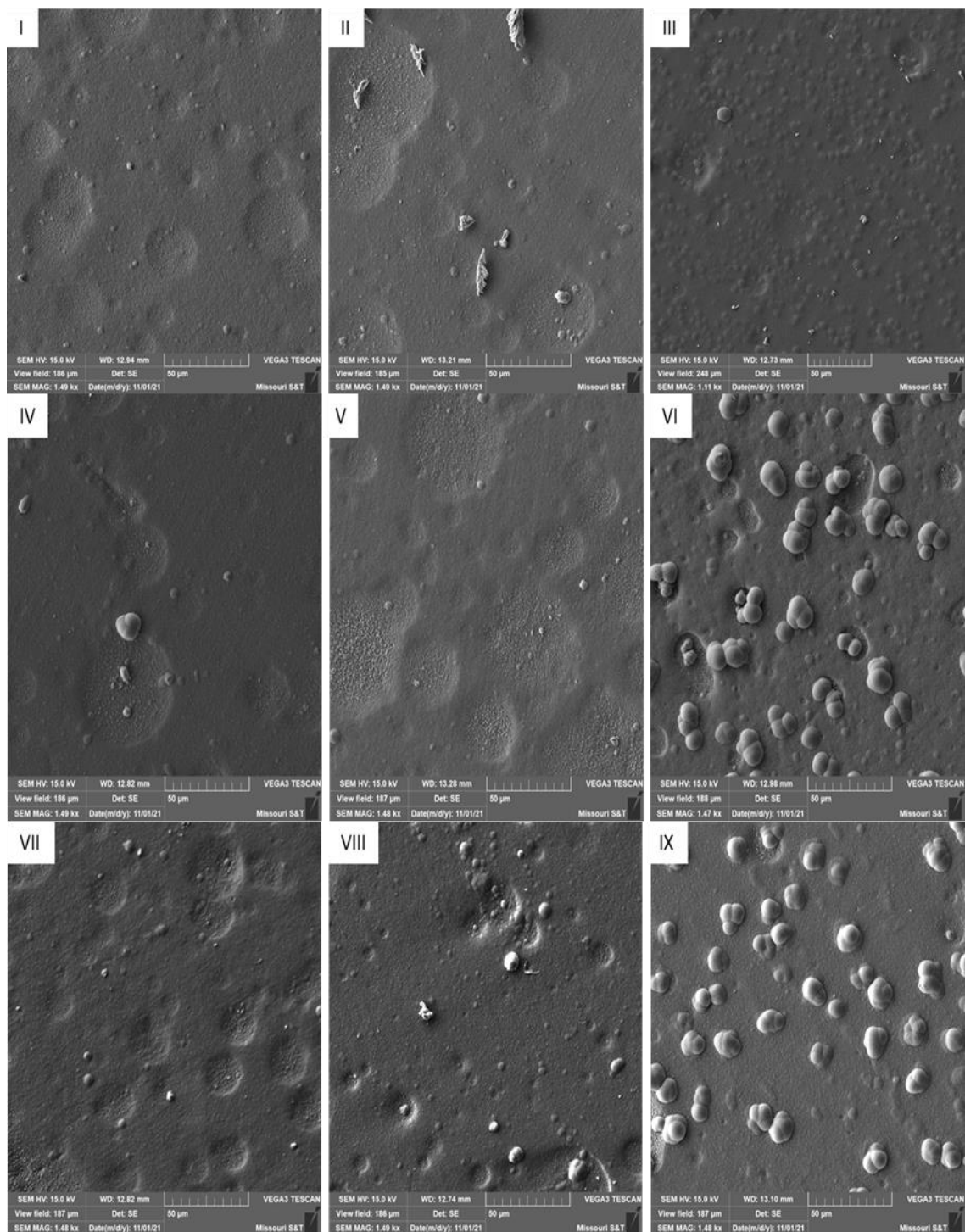


Figure 4. SEM images of Hull cell deposits at a current density of 305 A m^{-2} . Labels correspond to baths I to IX in Table 1. SE mode due to the topographical nature caused by the nodules.

The significant reduction in cathodic current densities as a function of electrode potential when additives were introduced to the plating bath is obvious and noteworthy.

The polarization curves produced with baths I to IX showed a gentle slope in reduction current (region E₁) followed by a rapid increase in reduction current (region E₂) with increasing potential. Other studies have attributed region E₁ to the formation of an iron oxide/hydroxide [17, 30] or zinc oxide/hydroxide [31, 32] layer on the cathode. The former reason seems unlikely in this study due to the pre-deposition of zinc on the working electrode prior to the polarization scan. The latter reason also appears improbable as the bath without additives did not depict similar behavior, respectively.

Region E₁ was believed to be caused by the adsorption of additives on the cathode. The adsorbed additives inhibit the rate of zinc reduction which allows for more compact deposits to form. This corresponds with results from the Hull cell plates which showed bright deposits at lower current densities for most plating baths.

The transition from region E₁ to region E₂ is believed to be related to the absorption strength of the additives on the zinc surface. Bath III (the brightest surface) has the most negative transitional potential while baths VI and IX (the duller surfaces) are the most positively shifted curves in region E₂. These shifts in potential (or energy) reveal the adsorption strength of the additives in the zincate baths with a more negative potential reveals a stronger bond and in turn the ability to produce smoother and brighter zinc surfaces.

The rapid increase in current observed in region E₂ is believed to be caused by the desorption of additives due to hydrogen evolution [28]. The slope observed in the polarization curve of the additive free bath is similar to the slopes region E₂ which

indicates the possibility of the rate of zinc reduction is no longer being controlled by the plating additives in the region.

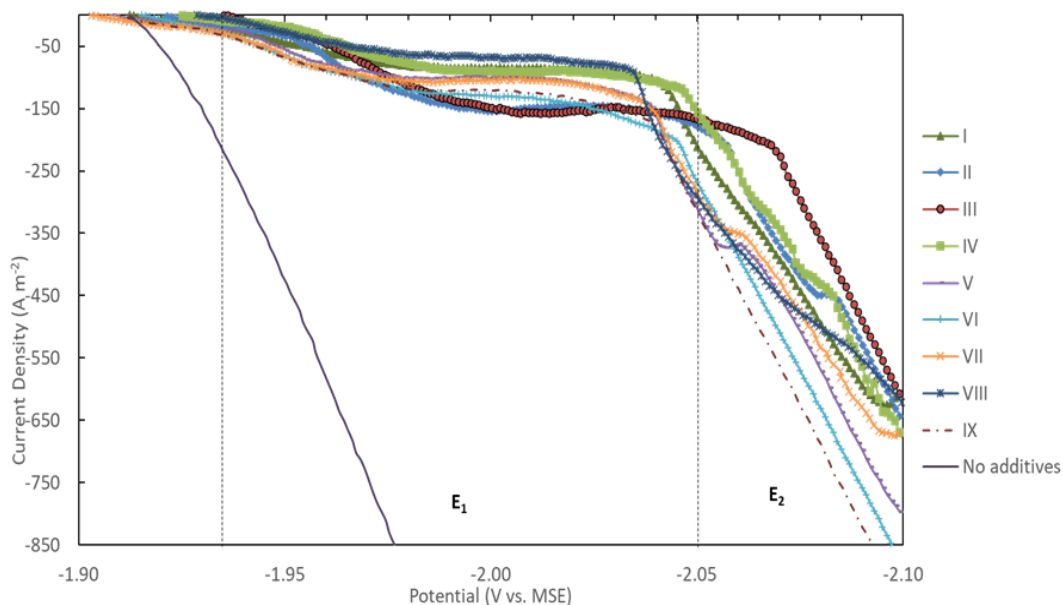


Figure 5. Cathodic polarization of plating baths with 37.5 g L^{-1} zinc and 210 g L^{-1} NaOH at $40 \text{ }^\circ\text{C}$ produced at a sweep rate of 1 mV s^{-1} . Bath additive concentrations are provided in Table 1.

3.4. THROWING POWER AND CATHODIC CURRENT EFFICIENCY

Throwing power (TP) as measured in a Haring Blum cell and cathodic current efficiency (CE) were measured at 305 A m^{-2} (anodic current density for Haring Blum cell and cathodic current density for two electrode cell for CE). Average TP and CE values measured for the nine plating baths with additives (see Table 1) are presented in Table 3.

The baths exhibited high CE due to the high concentrations of Zn and NaOH. Higher sodium hydroxide concentration decreased the hydrogen ion activity which resulted in high current efficiency.

Table 3. Throwing power and cathodic current efficiency for the plating baths with additive concentrations provided in Table 1 with a current density of 305 A m^{-2} at the anode in the Haring Blum Cell (throwing power) and cathode in two-electrode cell (current efficiency). Base electrolyte conditions were $37.5 \text{ g L}^{-1} \text{ Zn}$ and $210 \text{ g L}^{-1} \text{ NaOH}$.

Bath	Throwing power (%)	Current efficiency (%)
I	23	99
II	24	99
III	18	99
IV	30	99
V	37	98
VI	29	98
VII	32	98
VIII	30	99
IX	21	98

High zinc concentration increases the concentration of electroactive ion which results in improvement in the efficiency of zinc deposition [22, 33, 34]. At 305 A m^{-2} , the additives did not have any observable effect on CE.

An ANOVA of the throwing power results were performed with the findings presented graphically in Figure 6. The largest effect on throwing power was generated by the leveller concentration. While increasing the leveller concentration decreased the throwing power on average over the range studied, this effect was not statistically significant at $\alpha=0.05$. Throwing power has been found to depend on plating parameters such as zinc concentration, pH, current density, temperature, and plating duration [35-37]

and other studies have shown that additives can improve throwing power in zincate baths [38]. However, over the concentration ranges examined for these specific additives, no correlation was made between throwing power and additive concentrations or interactions.

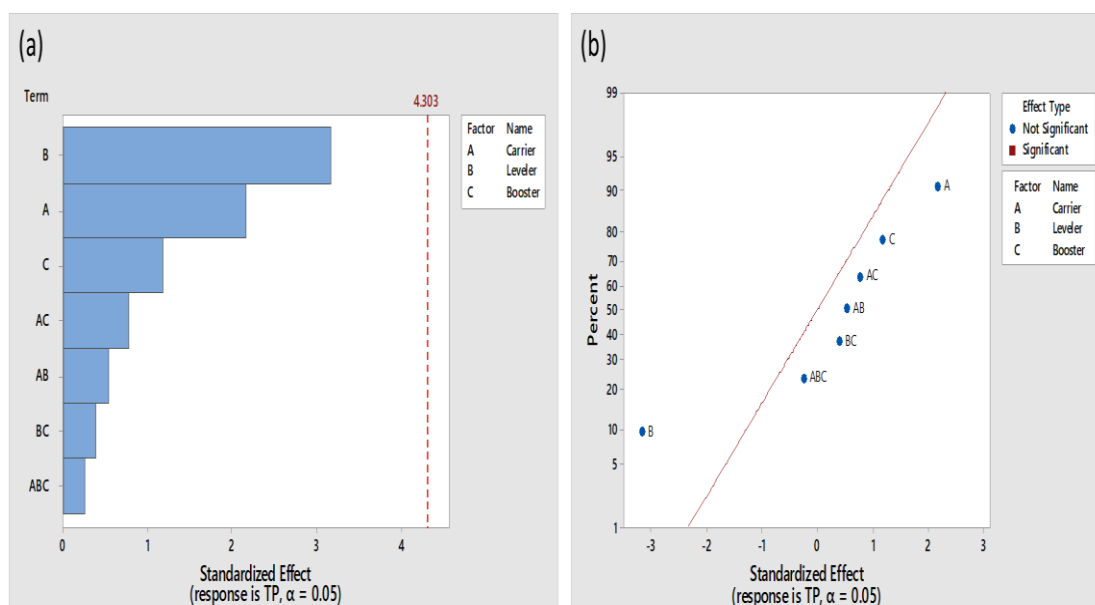


Figure 6. (a) Pareto chart and (b) Normal probability plot of the standardized effects of additives on throwing power.

4. CONCLUSIONS

The effects and interactions of three commercial additives (Eldiem carrier, Eldiem booster and Bright enhancer 2x) in a strong zincate bath ($Zn = 37.5 \text{ g L}^{-1}$ and $NaOH = 210 \text{ g L}^{-1}$) on deposit brightness and morphology, cathodic polarization, throwing power, and current efficiency were examined at higher concentrations than previously reported in the literature. Analysis of Hull cell deposits showed booster concentration and the

interaction between booster and carrier concentrations had significant effects on brightness within a current density range of 215 to 325 A m⁻². Increasing the booster concentration from 0.63 mL/L to 1.88 mL/L resulted in an average decrease in the gloss value of the deposits produced. The decrease in brightness was mitigated by increasing the concentration of carrier from 3.13 mL/L to 9.68 mL/L.

The concentrations of the additives had no statistically significant effect (at 95% confidence) on throwing power and current efficiency. Leveler concentration had the strongest effect on throwing power. Current efficiency at 305 A m⁻² was 98-99% for all conditions examined.

As expected, scanning electron microscopy revealed that rougher deposits correlated with duller (less gloss value) appearance. The presence of circular depressions indicate that hydrogen bubbles adhered to the zinc deposit during plating. Zinc nodules were commonly found in the circular depressions indicating that hydrogen evolution may be disrupting the additives' ability to produce smooth deposits.

Voltammetry indicated that additives significantly polarized the zinc deposition reaction. The potential at which additives desorb and/or hydrogen evolution commences appears to correlate with the presence of nodules on the zinc surface and thus deposit brightness on a qualitative basis.

REFERENCES

1. Smith, W.J., & Goodwin, F.E. (2017). Hot dip coatings, *Reference Module in Materials Science and Materials Engineering*. Elsevier, 2017.

2. Dallin, G.W. (2015). *Galvanizing-2015. Galvinfo Center – A Program Of The International Zinc Association.*
3. G., R., <https://www.portlandbolt.com/technical/faqs/hot-dip-galvanizing-vs-electrogalvanizing-zinc-plating> (Accessed on 10 November 2021).
4. Biddulph, C. (2012). Zinc electroplating. *Products Finishing, 1*, 106.
5. Vagramyan, T., Leach, J.L., & Moon, J.R. (1979). The structures of zinc electrodeposits formed at low current densities. *Journal of Materials Science, 14*(5), 1170-1174. doi:10.1007/BF00561301
6. Liang, Y.U.A.N., Ding, Z.Y., Liu, S.J., Shu, W.F., & He, Y.N. (2017). Effects of additives on zinc electrodeposition from alkaline zincate Solution. *Transactions of Nonferrous Metals Society of China, 27*(7), 1656-1664. doi:10.1016/S1003-6326(17)60188-2
7. Muralidhara, H.B., Naik, Y.A., Sachin, H.P., Achary, G., & Venkatesha, T.V. (2008). A study on brightening and corrosive resistance property of electrodeposited zinc in non-cyanide alkaline bath.
8. Schlesinger, M. & M. Paunovic. (2014). *Modern Electroplating.* Hoboken, UNITED STATES: John Wiley & Sons, Incorporated, 423-452.
9. Oniciu, L., & Mureşan, L. (1991). Some fundamental aspects of levelling and brightening in metal electrodeposition. *Journal of applied electrochemistry, 21*(7), 565-574.
10. Tietcha, G.F., Mears, L.L., Dworschak, D., Roth, M., Kluppel, I., & Valtiner, M. (2020). Adsorption and diffusion moderated by polycationic polymers during electrodeposition of zinc. *ACS Applied Materials & Interfaces, 12*(26), 29928-29936.
11. Hope, G.A, Brown, G.M., Schweinsberg, D.P., Shimizu, K., & Kobayashi, K. (1995). Observations of Inclusions of Polymeric Additives In Copper Electrodeposits By Transmission Electron Microscopy. *Journal of applied electrochemistry, 25*(9), 890-894.
12. Geduld, H. (1988). Zincate or Alkaline non-cyanide Zinc Plating in “Zinc Plating”. ASM International Metals Park, Ohio, 90-106.
13. Ravindran, V., Krishnan, R.M., & Muralidharan, V.S. (1998). Characteristics of an Alkaline Tartrate Zinc Plating Bath. *Metal finishing, 96*(10), 10-15.
14. Crotty, D., & Bagnall, K. (1988). Analysis methods for zinc plating brighteners. *Plat. Surf. Finish, 75*(11), 52-56.

15. Shanmugasigamani, & Pushpavanam, M. (2006). Role of additives in bright zinc deposition from cyanide free alkaline baths. *Journal of applied electrochemistry*, 36(3), 315-322. doi:10.1007/s10800-005-9076-9
16. Hsieh, J.C., Hu, C.C., & Lee, T.C. (2009). Effects of Polyamines on the Deposition Behavior and Morphology of Zinc Electroplated at High-current Densities in Alkaline Cyanide-free Baths. *Surface and Coatings Technology*, 203(20-21), 3111-3115. doi:10.1016/j.surfcoat.2009.03.035
17. Ortiz-Aparicio, J.L., Meas, Y., Trejo, G., Ortega, R., Chapman, T.W., & Chainet, E. (2013). Effects of organic additives on zinc electrodeposition from alkaline electrolytes. *Journal of Applied Electrochemistry*, 43(3), 289-300. doi:10.1007/s10800-012-0518-x
18. Naik, Y.A., & Venkatesha, T.V. (2003). A New Brightener for Zinc Plating From Non-cyanide Alkaline Bath. *Indian Journal of Engineering & Materials Sciences*, 10, p. 318-323.
19. Naik, Y.A., & Venkatesha, T.V. (2005). A new condensation product for zinc plating from non-cyanide alkaline bath. *Bulletin of Materials Science*, 28(5), 495-501. doi:10.1007%2FBF02711243
20. Chotirach, M., Rattanawaleedirojn, P., Boonyongmaneerat, Y., Chanajaree, R., Schmid, K., Metzner, M., & Rodthongkum, N. (2022). Systematic investigation of brightener's effects on alkaline non-cyanide zinc electroplating using HPLC and molecular modeling. *Materials Chemistry and Physics*, 277, 125567.
21. Pary, P., Bengoa, J.F., Conconi, M.S., Bruno, S., Zapponi, M., & Egli, W.A. (2017). Influence of organic additives on the behaviour of zinc electroplating from alkaline cyanide-free electrolyte. *Transactions of the IMF*, 2017. 95(2), 83-89.
22. Wanotayan, T., Kantichaimongkol, P., Chobaomsup, V., Sattawitchayapit, S., Schmid, K., Metzner, M., Chookajorn, T., & Boonyongmaneerat, Y. (2020). Effects of Chemical Compositions on Plating Characteristics of Alkaline Non-Cyanide Electrogalvanized Coatings. *Nanomaterials*, 10(11), 2101. doi:10.3390/nano10112101
23. Scott, M., & Moats, M. (2020). Optimizing Additive Ratios in Alkaline Zincate Electrodeposition. In *PbZn 2020: 9th International Symposium on Lead and Zinc Processing*, Springer, Cham: 123-131.
24. Scott, M. (2020). Effect of Carriers, Brighteners, and Levelers on Zinc Electrogalvanizing in Alkaline Zincate Solutions. Master of Science thesis, Missouri University of Science and Technology, Missouri.
25. Antony, J. (2003). *Design of Experiments for Engineers and Scientists*. Butterworth-Heinemann, Burlington, MA;Oxford: 60-65

26. Hunter, R.S. (1937). Methods of Determining Gloss. *NBS Research paper RP*, 958.
27. Gabe, D.R. (2002). Test cells for plating. *Metal Finishing*, 100, 579-586.
[https://doi.org/10.1016/S0026-0576\(02\)82059-1](https://doi.org/10.1016/S0026-0576(02)82059-1)
28. Hsieh, J.C., Hu, C.C. & Lee, T.C. (2008). The Synergistic Effects of Additives on Improving the Electroplating of Zinc Under High Current Densities. *Journal of The Electrochemical Society*, 155(10), D675.
29. Adam Blakeley, M. <https://www.pfonline.com/articles/plating-clinic-improving-acid-zinc-coverage-and-brightness>. (Accessed 16 November 2021).
30. De Carvalho, M.F., Rubin, W. & Carlos, I.A. (2010). Study of the Influence of the Polyalcohol Mannitol on Zinc Electrodeposition from an Alkaline Bath. *Journal of applied electrochemistry*, 40(9), 1625-1632. doi:10.1007/s10800-010-0148-0
31. Gomes, A., & da Silva Pereira, M.I. (2006). Pulsed electrodeposition of Zn in the presence of surfactants. *Electrochimica Acta*, 51(7), 1342-1350.
doi:10.1016/j.electacta.2005.06.023
32. Casanova, T., Soto, F., Eyraud, M. & Crousier, J. (1997). *Hydrogen Absorption During Zinc Plating on Steel*. *Corrosion science*, 39(3), 529-537.
[https://doi.org/10.1016/S0010-938X\(97\)86101-X](https://doi.org/10.1016/S0010-938X(97)86101-X)
33. Ouakki, M., El Fazazi, A. & Cherkaoui, M (2019). Electrochemical Deposition of Zinc on Mild Steel. *Mediterranean Journal of Chemistry*, 8(1), 30-41.
doi:10.13171/mjc8119021318mo
34. Gamburg Y.D. & Zangari G. (2011). *Theory and Practice of Metal Electrodeposition*. Springer Science & Business Media.
35. Ibrahim, M.A.M. (2000). Improving the throwing power of acidic zinc sulfate electroplating baths. *Journal of Chemical Technology & Biotechnology: International Research in Process, Environmental & Clean Technology*, 75(8), 745-755. doi:10.1002/1097-4660(200008)75:8<745::AID-JCTB274>3.0.CO;2-5
36. Sekar, R., Jagadesh, K.K., & Ramesh Babu, G.N.K. (2015). Role of Amino Acids on Electrodeposition and Characterisation of Zinc from Alkaline Zincate Solutions. *Transactions of the IMF*, 93(3), 133-138.
doi:10.1179/0020296715Z.0000000000239
37. Babu, G.R., Devaraj, G., & Ayyapparaj, J. (1998). Studies on Non-cyanide Alkaline Zinc Electrolytes. *Journal of Solid State Electrochemistry*, 3(1), 48-51.
38. Kavitha, B., Santhosh, P., Renukadevi, M., Kalpana, A., Shakkthivel, P., & Vasudevan, T. (2006). Role of organic additives on zinc plating. *Surface and Coatings Technology*, 201(6), p. 3438-3442. doi:10.1016/j.surfcoat.2006.07.235

II. SIMULATION OF CURRENT DENSITY DISTRIBUTION IN ELECTROGALVANIZATION CELL

Abdul J. Mohammed, Michael Moats*, Arezoo Emdadi and Yijia Gu

Materials Research Center
Missouri University of Science and Technology
Rolla, MO, USA 65409

*Corresponding author, moatsm@mst.edu

ABSTRACT

Computer simulations can be utilized to predict the response of electrochemical cells to input parameters. A validated plating model can be used optimize complex industrial plating operations improving production yield and process efficiency. In this study, an electrodeposition computer model was developed using experimentally generated fundamental electrochemical data for a highly concentrated alkaline zincate electrogalvanizing plating bath. COMSOL multiphysics software was used to build a two-dimensional computational model involving mass transfer and electrode reactions. The model was validated by comparing the predicted current density distribution with experiment data for a rotating cylinder Hull cell. The model was further tested against plating thickness data from a custom build laboratory plating cell which was built to simulate an industrial tube plating operation. The COMSOL model produced results similar to what was expected based on industrial observations. Unfortunately, the experimental data did not correlate well with the model results due to control of tube position during the plating experiments.

1. INTRODUCTION

Electro galvanization is the preferred method over hot-dip galvanization when uniform zinc coating is required in the protection of steel from corrosion [1]. The uniformity of coatings from an electroplating solution is commonly referred to as the levelling capability of the solution. Levelling is the ability of an electroplating bath to produce deposits thicker in small recesses and thinner on small protrusions leading to a smooth surface in a localized area[2]. Levelling can be due to geometric levelling which is produced by uniform current distribution created by appropriate cell design or higher throwing power baths. Reduction in current distribution variation results in a more uniform coating, less re-work parts and ultimately a higher throughput of a plating facility. Levelling at the sub-millimeter scale on the other hand is due to the adsorption of plating additives on protrusion to promote deposition at recesses [3].

The study of current distribution on electroplated parts is important since it influences the appearance and uniformity of coatings. Non-uniformity can be caused by electric potential differences generated by the shape of part being coated and/or geometry of the cell [4]. The most common quality control cell used to examine deposit thickness and appearance of metal electrodeposits as a function of current density is the Hull cell [5].

The Hull cell is a simple tool that is used to determine the performance of plating baths over a wide current density range in a single quick test. Process control parameters such as optimum additive concentrations and current density range [6-8] can be

ascertained using a Hull cell. These results can then be applied by someone skilled in the plating arts to control an electrogalvanizing operation.

As shown in Figure 1, a Hull cell is a trapezoidal shape cell with the cathode slanted at an angle of 37° relative to the anode [9]. The varying distance between the anode and the cathode results in a variable current density across the cathode. Equation 1 represents the current density distribution across the cathode [10].

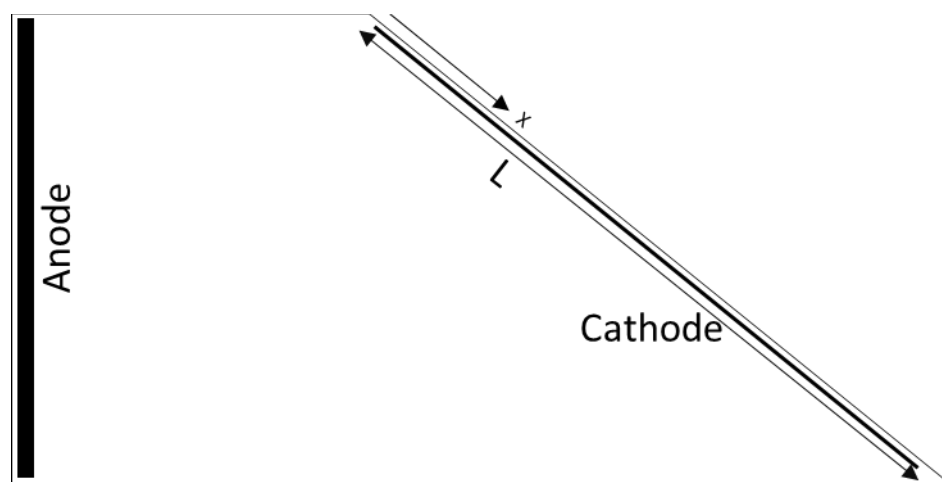


Figure 1. A schematic diagram of a standard Hull cell used to evaluate electroplating coating thickness and appearance [11].

$$i_{(x)} = I_{\text{appl}}(a - b \log L) \quad (1)$$

$i_{(x)}$ = current density at point x along the cathode from the zero point where the cathode is closest to the anode

I_{appl} = total current applied

L = length along the cathode

a and b = constants based on units used (for cm and $A \text{ cm}^{-2}$ a is 5.1 and b is 5.24)

and the geometry of a 267 mL standard Hull cell.

The Hull cell is constructed of insulating materials such as Lucite or polypropylene based on the electrolyte to be studied.

Standard Hull cells are widely used qualitatively for process control due to irreproducible mass transfer [12]. However, mass transport is important in obtaining sufficient quantitative information about the electroplating process. Some manufacturers include air sparging in Hull cell to simulate agitated plating baths, but this does not provide mass transfer conditions [5].

The rotating cylinder Hull Cell (RCHC) was developed to study electroplating under controlled hydrodynamic conditions to facilitate a better understanding of plating processes [5]. A RCHC permits for the measurement of nonuniform current distribution, mass transport and the throwing power of a plating bath in a single experiment. As shown in Figure 2, the cell consists of a rotating cylinder electrode mounted on a rotating shaft as cathode. An insulating cylindrical wall is placed between the cathode and a cylindrical outer anode to produce a nonuniform current distribution along the cathode length[13].

Even with quality control devices like the Hull cell and RCHC, control of complex industrial plating baths can be challenging. Direct experimentation in industrial systems can also be impractical and/or costly. Hence, the allure of using computer simulations for plating process development is enticing. A validated electroplating model that can predict the performance of industrial plating cells could be used to simulate process design changes to enhance the success of experimentation and improve the operation.

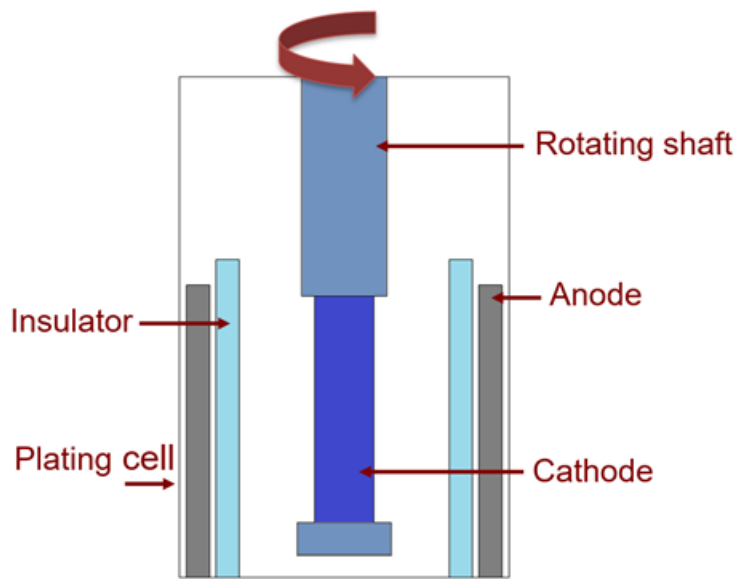


Figure 2. A 2-D schematic cross-section of a rotating cylinder Hull cell (RCHC) showing the anode (counter electrode), the cathode (working electrode) on a rotating shaft and an electrical insulator.

In this study, an electroplating model for a high concentration alkaline zincate electrogalvanizing bath was created. The aim of the model was to predict the current distribution during electrogalvanizing of steel conduits. To ascertain the validity of the model, tests were run in laboratory cells to measure current density variation experimentally.

The model was created using COMSOL's Multiphysics software. COMSOL Multiphysics is a finite element-based software that can be used to study the current and potential distribution along the cathode in an electrochemical system [11, 14, 15]. Electrochemical fundamental data were generated for the alkaline zincate electrogalvanizing plating bath to serve as inputs for the electrodeposition model. The electroplating model was validated using experimental data from a RCHC. The model

was then compared to zinc electrogalvanizing results from a custom-built laboratory cell with a moving steel conduit tube.

2. EXPERIMENTAL

2.1. PLATING BATH

Plating baths or electrolytes were prepared by dissolving high purity zinc balls (Belmont Metals) into a NaOH solution. Analytical reagent grade NaOH (Fisher Chemicals) and deionized and distilled water (18.3 M Ω .cm) were used to prepare the solution. The zinc and sodium hydroxide concentrations were determined by titration and then diluted to 37.5 g L⁻¹ zinc and 210 g L⁻¹ NaOH using de-ionized water. The resulting solution was purified using zinc dust cementation and mild electrolysis [16].

Three commercial plating additives - Eldiem Carrier, Eldiem booster and Bright Enhancer 2x at concentrations of 1.29 mL L⁻¹, 0.26 mL L⁻¹, and 0.51 mL L⁻¹ respectively, were used in this study without further purification. The plating additives were added to the electrolyte and preheated for 60 minutes prior to each experiment. All experiments were performed at 40°C (\pm 2°C).

2.2. CATHODIC POLARIZATION

Cathodic polarization (current vs. potential) measurements were performed in a three-electrode cell using the alkaline zinc solution with additives to generate fundamental electrochemical data needed as inputs for the plating model. The electrochemical tests were controlled using a Gamry 3000 potentiostat.

A rotating 316L stainless-steel working electrode disc (5mm diameter), platinum mesh counter electrode and mercury/mercury sulfate (MSE) reference electrode were used. The reference electrode was placed in a Luggin tube filled with the test solution. The tip of the Luggin tube was 1.5 cm from the surface of the working electrode. The working electrode was rotated at 500 rpm to control the mass transport conditions. The solution was sparged with nitrogen gas for 10 minutes to remove oxygen prior to each experiment. The working electrode was pre-plated with zinc for 5 minutes using a current density of 320 A/m^2 prior to employing linear sweep voltammetry (LSV). The working electrode potential was scanned from -1.9 to -2.1 V vs. MSE (0.64 vs. SHE at $25 \text{ }^\circ\text{C}$) at a scan rate of 10 mV/s to generate cathode polarization data.

2.3. ROTATING CYLINDER HULL CELL

Triplicate experiments were conducted in a RCHC to measure the current distribution on a rotating stainless-steel cylinder to validate the electroplating model with a well-defined plating system, which has been modelled previously with other electrolyte systems.

The RCHC configuration uses an outer anode (a 7 cm diameter mild steel pipe) and a concentric inner stainless-steel cylinder (1.6 cm diameter). The stainless-steel cylinder was mounted to a rotating shaft. An insulating cylindrical wall (6.4 cm diameter) was placed between the anode and cathode to produce a non-uniform current distribution along the cathode length. The cylinder was rotated at 700 rpm to produce turbulent conditions which are observed in industrial practice. An average cathode current density

of 323 A/m^2 was applied using a 3000 Gamry potentiostat for a period of 720s to grow a zinc deposit thick enough to measure by weight.

The zinc deposit was divided into six sections and then each section was dissolved in 50 % HCl. The loss in mass was used to determine the mass of the deposit after each section was dissolved. The current density for each section was then calculated from the coating mass using Faraday's law with a current efficiency of 90%. The current efficiency was determined by experiments using a rotating cylinder cell with the same plating conditions as the RCHC but without the insulator.

2.4. LABORATORY TUBE PLATING CELLS

Figure 3 shows the custom laboratory tube plating cell fabricated for this study. The plating cell constitutes all the components of an industrial plating operation but at a laboratory scale. Polypropylene was selected for the fabrication of all non-conductive parts due to its resistance to high temperatures and strong alkaline conditions. The plating tank is a 227 L polypropylene tank with a dimension of 0.9 m X 0.5 m X 0.5 m. At the bottom of the tank was a 0.8 by 0.4 m mild steel grating which served as the anode. The cathode which was suspended at a height of 0.3 m from the anode and was made of copper strips of 1.8 mm thickness embedded in a cylindrical polypropylene rod.

The tank is heated by liquid-to-liquid heat transfer by pumping hot water through copper coils running along the vertical walls of the tank. Polypropylene mesh has been put in place to prevent an electrical arc due to accidental contact of electrically polarized tubes to heating coils which can result in a hole in the cooling coils.



Figure 3. Laboratory tube plating cell.

A drive system moves suspended hooks forward and reverse through the tank to simulate the long continuous movement of conduits during electrogalvanization in industrial tanks. The drive system was powered by a 1800rpm dc motor (Dayton 4Z528) which is controlled by a speed controller with a range of 0.30 to 6.1 m/min (Dayton 6X65E). Experiments were run using 40 cm long conduits.

The conduits were cleaned using an alkaline cleaner at 65 °C to remove oil and grease. The grease-free conduits were rinsed in deionized water and then dipped in 50 % HCl to get rid of oxide layers and activate the surface.

Plating was performed at an average cathode current density and plating duration of 323 A m⁻² and 12 mins, respectively. Electric power was supplied using an Extech 382275. After plating, the conduits were rinsed with deionized water, dipped in 0.5%

nitric acid for 10 seconds and then rinsed again with deionized water. The rinsed conduit was air dried to avoid water stains on the zinc coating.

Plated conduits were divided into 16 sections and thickness of the various sections were measured using a DeFelsko Positector6000 coating thickness gage. The current density for each section was then calculated from the coating thickness to determine the current distribution along the cathode. The calculated current density used Faraday's law and a current efficiency of 90%.

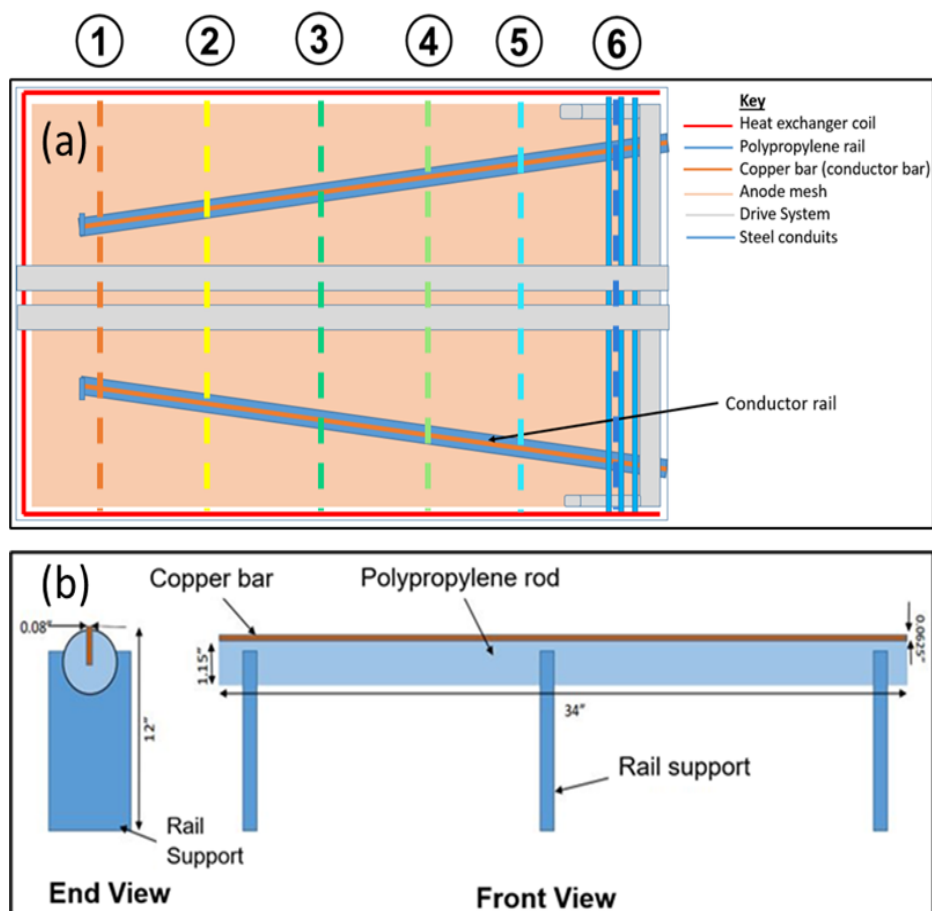


Figure 4. Schematic drawing of the laboratory setup; (a) top view of the tank, and (b) the conductor rail. The six positions for which computer simulations were calculated are marked with dashed lines.

3. COMPUTATIONAL MODELLING OF ALKALINE ZINCATE ELECTROGALVANIZING

The throwing power of alkaline zincate electrogalvanizing baths are not as strong traditional cyanide baths [17]. The throwing power of the alkaline zincate bath used in this study was reported previously [16] as 18-40% based on Haring-Blum cell measurements. This throwing power can cause thickness variation during industrial zinc plating of steel tubes.

A computational model for electrogalvanizing (EGL) was developed for an alkaline zinc bath to allow for the prediction of local current density distribution along a cathode in an EGL system. For this purpose, COMSOL Multiphysics software was utilized. Within COMSOL, the electrochemistry module with secondary current distribution sub-module [18] was employed. This module allows the simulation of the electrochemical reactions at the interface between a metal electrode and an electrolyte, as well as the transport of ions and neutral species within the electrolyte. To simulate the Zn electroplating process, mass transfer, electrochemistry, and electrode reactions were considered.

The electroplating model was developed using experimentally measured solution resistance and cathode polarization data. The computational model was developed to ensure reasonable prediction of the current density data generated in the rotating RCHC. Then, the model was utilized to simulate the larger laboratory tube plating cell for comparison with experimental results.

3.1. ROTATING CYLINDER HULL CELL (RCHC) MODELLING

A 2D computational model was developed to calculate the current density distribution along the cathode for a RCHC setup. A 2D slide of half of the RCHC was appropriate to capture the current distribution due to the symmetry of the cylindrical design of the RCHC. This model was utilized to understand the boundary/initial conditions, as well as, to find the appropriate solver parameters for a stable and convergence solution. The geometry of the RCHC and the finite element mesh distribution of the 2D axisymmetric RCHC model in COMSOL are presented in Figures 5(a) and (b), respectively. The RCHC modelling parameters are summarized in Table 1.

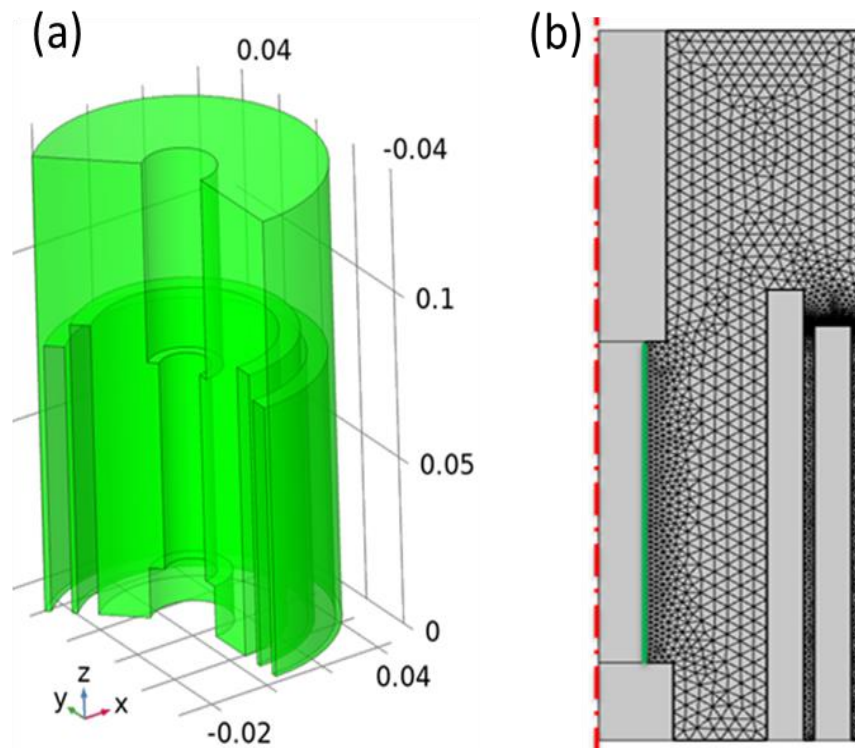


Figure 5. (a) The geometry of RCHC and (b) the finite element mesh distribution for the 2D axisymmetric RCHC model.

Table 1. The RCHC operation parameters values and descriptions.

Parameter	Value
Electrolyte conductivity	20.9 [S/m]
Operation temperature	313 [K]
Equilibrium potential for cathode	-0.64 [V]
Cathode average current	325 [A/m ²]
Equilibrium potential for anode	0.76 [V]
Transfer coefficient (anode)	0.5
Exchange current density(anode)	15.07 [A/m ²]
Molar mass for Zn	65.38 [g/mole]
Density for Zn	7140 [kg/m ³]

3.2. LABORATORY TUBE PLATING CELL

As the laboratory tube plating cell (Fig. 3) is more geometrically complex, a two-dimensional (2D) geometry configuration was developed to facilitate the convergence of numerical simulations. Figure 4 shows a schematic drawing of the laboratory setup. Figure 6(a) shows a schematic cross-section of the lab-setup plating cell with 6 different positions of polypropylene along the cell. The six positions were used to generate current distributions based on the location of a tube in the cell as it rolls along the cathode rails. The simulation results from the six positions were averaged to produce an average current distribution on the tube as it rolled back and forth on the cathode rails during the physical experiment. A free triangular mesh was utilized with a user-defined finer mesh in the vicinity of the lower surface of the cathode to get a more precise current density calculation (Figure6(b)). The model input parameters were the same as those used in the RCHC model (Table 1).

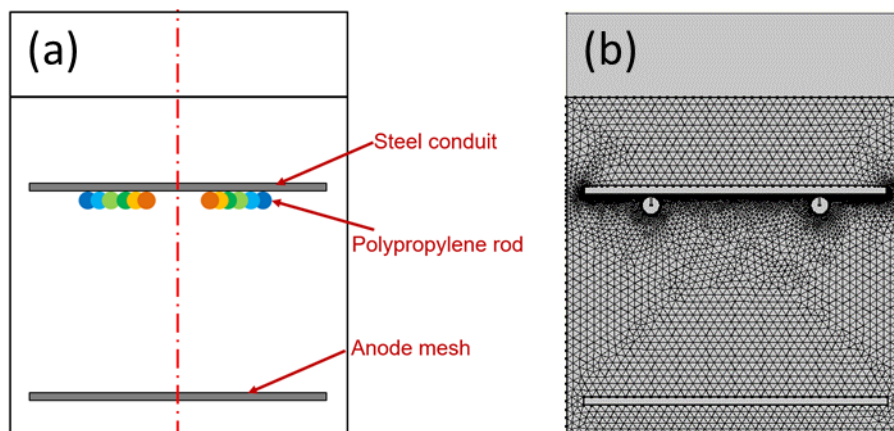


Figure 6. (a) The schematic cross-section of the lab-setup plating cell, (b) the mesh size and distribution used in the finite element modeling.

4. RESULTS AND DISCUSSION

4.1. FUNDAMENTAL ELECTROCHEMICAL DATA

Figure 7 shows the cathode current density (i) vs. the absolute value of the overpotential $|E-E_0|$ as measured in a three-electrode cell. The blue dots are the measured data which indicates the Butler-Volmer equation is not valid. Equation (2) is a fitted piecewise function over the experimental data, and it is presented as the red curve in Figure 7.

4.2. RCHC SIMULATION AND EXPERIMENTAL RESULTS

To determine the local current distribution along the cathode and validate the model, the empirical equation in Eq. (2) was used for cathodic polarization and Butler-Volmer Equation for anode kinetics. Equation 2 was inputted into COMSOL as a user-defined equation for current density vs overpotential along the cathode. The initial potential for the cathode was assumed to be -0.64 V (potential for the reverse reaction vs.

SHE). For the electrolyte, the potential was supposed to be 0 V at the beginning of the simulations. An average current density of 325 A/m² was considered as the boundary condition along the cathode. The electric potential boundary condition along the anode is assumed to be 0V.

The electroplating model results are compared to experimental results from the RCHC experiments in Figure 8(a) The position of each deposit section in the RCHC is depicted in Figure 8(b). The computational results agreed with the measured values within experimental error indicating the model sufficiently reproduced zinc plating from the alkaline zincate bath.

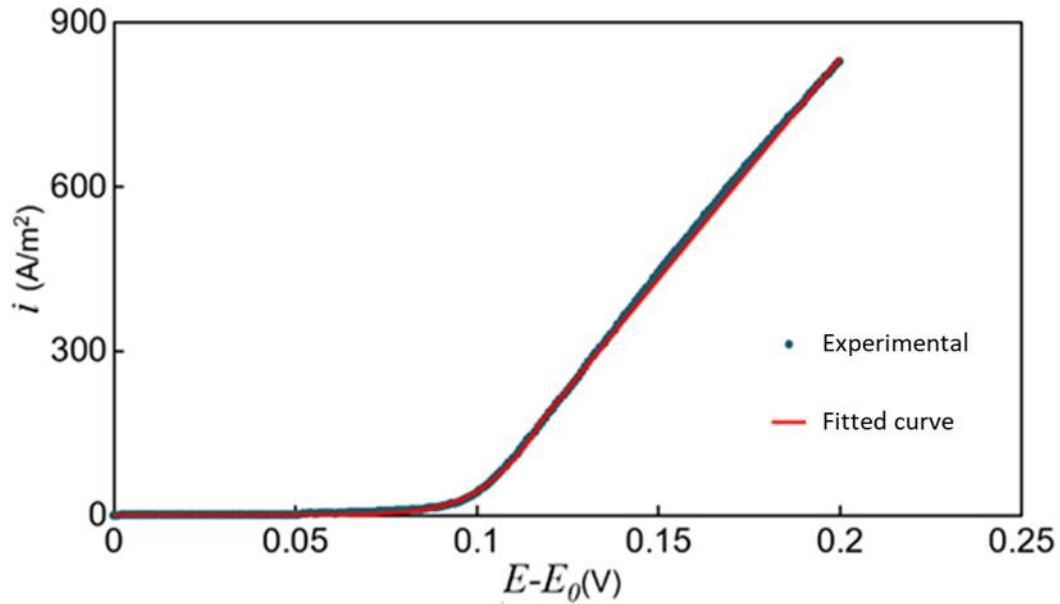


Figure 7. Cathode current density (i) vs overpotential ($E-E_0$). The blue dots are the lab measurement data. The red curve is the empirical piecewise fitted function.

$$i = \begin{cases} 0.02e^{(-0.72 + 4.82E^* + 1575.67E^* - 7652.22E^{*3})} & (E^* = E-E_0) \leq 0.12V \\ 8068.61E^* - 777.04 & (E^* = E-E_0) > 0.12V \end{cases} \quad (2)$$

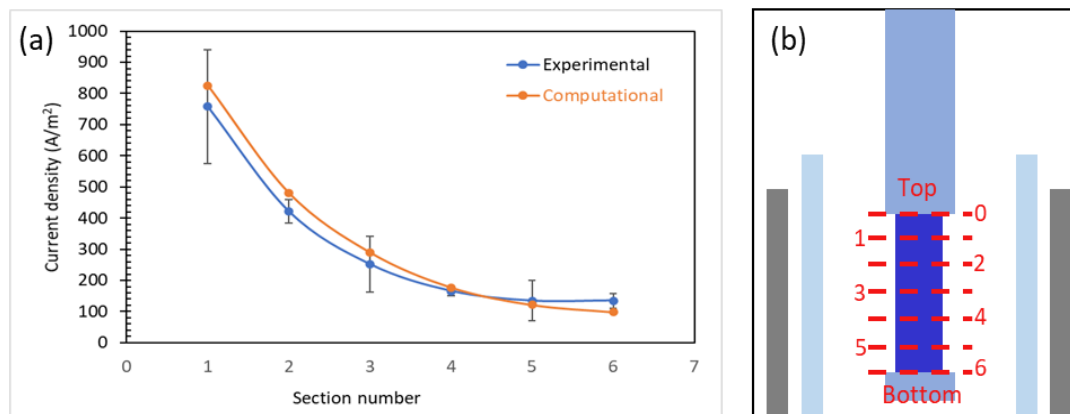


Figure 8. The experimental measurements (error bars are +/- 2 standard deviation) and the computational calculation of cathode current density for RCHC, and (b) a schematic of each section position along the cathode.

4.3. LABORATORY TUBE PLATING CELL SIMULATION AND RESULTS

As the electroplating model adequately predicted the current distribution in the RCHC for alkaline zincate electrogalvanizing, it was used without modification to simulate the current density distribution in the laboratory tube plating cell.

The streaming distribution of the electrolyte potential from the anode to the cathode is presented in Figure 9. The difference in electrical potential between the cathode and anode is about 3V, which is similar to the cell voltage for the experimental lab cell during operation. This was the first validation test of the computer simulation with experimental data.

Figure 10 shows the simulated current distribution on the bottom surface of the tube for six different positions of the conduction rail within the cell (Figure 6 (a)). As expected, the simulation results reveal a drop in current density when the tube is over the conducted rails due to the insulating effects of the polypropylene (Figure 10). The average current distribution for the six positions was calculated and is displayed in Figure

10 (dashed line). As the tube rolls along the conductor rails as the drive mechanism pushes or pulls the tube during the experiment, it was hoped that the average current density would adequately simulate experimental results. This would allow for less computer simulation time instead of creating the need to model in 3D with a moving part.

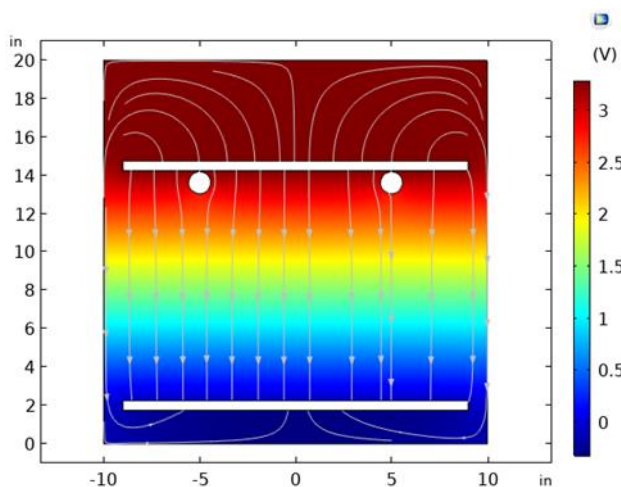


Figure 9. The stream distribution of the electrolyte potential.

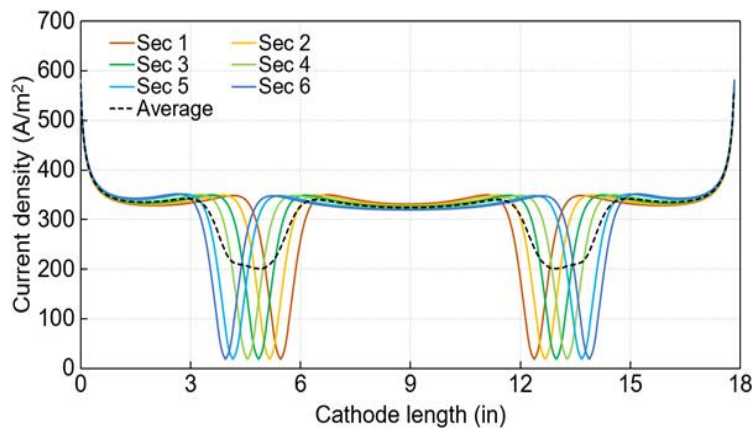


Figure 10. Computational results for the distribution of the current density along the simulated tube for 6 different positions on the conducted rail and an average of the values.

The average calculated current density from the COMSOL model is compared to experimental data from the laboratory plating cell in Figure 11. The model predicted the current density range (200 to 450 A m⁻²) along the tube which was expected based on the commercial operation being simulated. The general shape of the current density distribution is also consistent with industrial measurements of zinc coating thickness. However, the current density distribution measured at the various sections of the laboratory plated tubes differs from the computational values. It can be observed that the current at one end of the tube is higher than the other which makes the experimental current distribution asymmetrical.

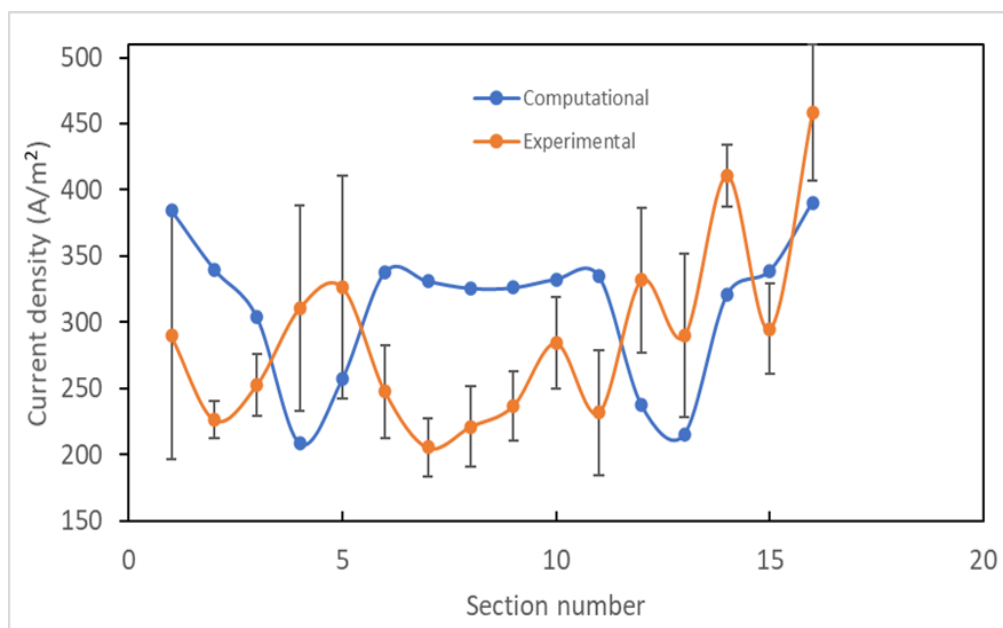


Figure 11. Computational and experimental results for the distribution of the current density along the tube.

The difference between the experimental and model results are believed to be caused by the movement of tube perpendicular to the rails during the electrogalvanization

experiment. Skewing of the tubes towards one of the rails due to solution flow resistance and the movement of the hooks affected the symmetry of the current distribution. Figure 12 shows rail marks formed on electrogalvanized tubes due to contact with the cathode rails. Symmetrical movement of the tube at the beginning of the process results in formation of point 1 and 2 while point 3 is formed due to the shift towards one of the rails. This indicates that the tube shifted to the right (as pictured) during the operation.

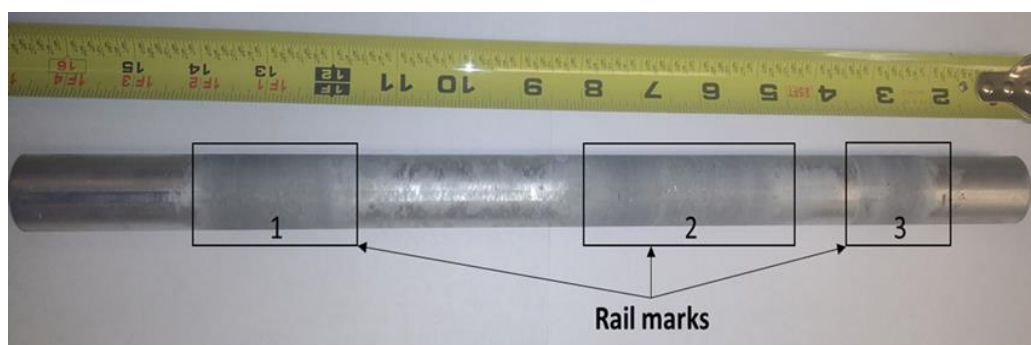


Figure 12. Tube plated from custom built laboratory plating cell. Points 1, 2 and 3 shows the rail marks due to contact to the cathode during the electrogalvanization process.

5. CONCLUSIONS

Computational models of a RCHC and a custom-built laboratory tube plating cell were built using COMSOL Multiphysics software to determine the current distribution in a unique zincate bath. Model developed from electrochemical data was validated by a RCHC. The simulated current density distribution correlated well with the RCHC experimental data.

The same model was then used to simulate a more complex laboratory-built cell. Despite the model predicting the current density range for the laboratory plating cell, there were variations between the measured and computational values at the various section of the plated tubes. The variations in current density were due to the shift in tubes from the original central position during the electroplating process.

Modifications must be made to the laboratory plating set up to produce a more symmetrical current distribution as assumed in the building of the model. Also, a more complex 3D model that involves the complete hydrodynamic conditions within the cell as well as the moving action of the tubes to account for the shift in tube position will produce a more accurate model of the system.

REFERENCES

1. G., R., <https://www.portlandbolt.com/technical/faqs/hot-dip-galvanizing-vs-electrogalvanizing-zinc-plating/> (Accessed 10 November 2021).
2. Thomas, J.D. (1956), Leveling, definition, measurement and understanding. *Proc. Amer. Electropl. Soc.*, **43**, 60.
3. Kardos, O. & Foulke, D.G. (1966), Advances in electrochemistry and electrochemical engineering. *Interscience Publishers*, 2, 145.
4. Dukovic, J.O. (1990), Computation of current distribution in electrodeposition, a review. *IBM Journal of Research and Development*, 34(5), 693-705. doi.org/10.1147/rd.345.0693
5. Teeratananon, M., Pruksathorn, K., Damronglerd, S., Dupuy, F., Vergnes, H., Fenouilletc, B. & Duverneuic, P. (2004), Experimental investigation of the current distribution in Mohler cell and Rotating Cylinder Hull cell. *Electrochimica Acta*, 30, 375-381.

6. Onkarappa, N.K., Satyanarayana, J.C.A., Suresh, H. & Malingappa, P. (2020), Influence of additives on morphology, orientation and anti-corrosion property of bright zinc electrodeposit. *Surface and Coatings Technology*, 397, 126062. doi.org/10.1016/j.surfcoat.2020.126062
7. Naik, Y.A. & Venkatesha, T.V. (2003), A new brightener for zinc plating from non-cyanide alkaline bath. *Indian Journal of Engineering & Materials Sciences*, 318-323.
8. Scott, M. & Moats, M. (2020), Optimizing additive ratios in alkaline zincate electrodeposition. In *PbZn 2020: 9th International Symposium on Lead and Zinc Processing*, Springer, Cham, 123-131. doi.org/10.1007/978-3-030-37070-1_11
9. Schlesinger, M., M. Paunovic & M. Paunovic (2014), *Modern electroplating*. Hoboken, UNITED STATES: John Wiley & Sons, Incorporated, 423-452.
10. Gabe, D.R. (2002), Test cells for plating. *Metal Finishing*, 100, 579-586. doi.org/10.1016/S0026-0576(02)82059-1
11. Lima, F., Mescheder, U. & Reinecke, H. (2012), Simulation of current density for electroplating on silicon using a Hull cell. *Solar Cells*, 6, 7.
12. AT&T Bell Laboratories, M.H., N.J. (1993), Electroplating test cell.: p. 5268087.
13. Madore, C. & Landolt, D (1993), The rotating cylinder Hull cell: design and application. *Plating and Surface Finishing*, 80, 73.
14. Tong, L. (2011), Tertiary current distributions on rotating electrodes. *Proceedings of the COMSOL Conference*, Tokyo, Japan.
15. Low, C.T.J., Roberts, E.P.L. & Walsh, F.C. (2007), Numerical simulation of the current, potential and concentration distributions along the cathode of a rotating cylinder Hull cell. *Electrochimica Acta*, 52(11), 3831-3840. doi.org/10.1016/j.electacta.2006.10.056
16. Mohammed, A.J. & Moats, M (2022). Effects of Carrier, Leveller, and Booster Concentrations on Zinc Plating from Alkaline Zincate Baths. *Metals*, 12, 621. https://doi.org/10.3390/met12040621
17. Loto, C.A. (2012), Electrodeposition of zinc from acid based solutions: a review and experimental study. *Asian Journal of Applied Sciences*, 5(6), 314-326.
18. https://www.comsol.com/documentation. (Accessed 28th July 2020).

SECTION

3. CONCLUSIONS AND RECOMMENDATIONS

3.1. CONCLUSIONS

Effects of concentrations of commercial additives: carrier, leveler and booster in high concentration alkaline zincate bath were studied. Only the booster concentration and the interaction between booster and carrier concentrations produced a statistically significant effect on deposit brightness over the ranges studied. Additive concentrations did not have a statistically significant effect on throwing power or current efficiency. Baths with additives showed significant cathodic polarization compared to an additive free bath.

A COMSOL model was developed by project collaborators to predict the current distribution in two laboratory cells. Fundamental polarization data for zinc deposition from the highly concentration alkaline zincate system with additives used in this study were measured. The data led to empirical formulae used in the model. The COMSOL model was successfully validated using a rotating cylinder Hull cell. The model was able to predict the current density range in a custom built laboratory tube plating cell with a much more complex geometry. However, there was significant variation between the computational and measured current density values due to experimental error.

3.2. RECOMMENDATIONS

Further studies should be carried out in plating at high current density regions without causing the desorption of additives due to hydrogen gas evolution. Additives with hydrogen gas inhibition properties might immensely improve deposit properties even at high current density regions.

The laboratory tube plating cell should be modified to prevent the horizontal movement of the conduits during the experiment. COMSOL model will then be validated in the more complex system.

After final validation, the COMSOL could be used to optimize existing electrogalvanizing operations that use this alkaline zincate plating system.

BIBLIOGRAPHY

1. Dallin, G.W. (2015). *Galvanizing-2015*. Galvinfo Center – A Program Of The International Zinc Association.
2. Naik, Y.A., Muralidhara, H.B., Sachin, H.P., Achary, G., & Venkatesha, T.V. (2008). A study on brightening and corrosive resistance property of electrodeposited zinc in non-cyanide alkaline bath. *Indian Journal of Chemical Technology*, 15, 259-265.
3. *Zinc Coatings (2011) - A Comparative Analysis of Process and Performance Characteristics*. American Galvanizers Association.
4. Achary, G., Mathias, D.P. & Nayaka, Y.A. (2017). Electrodeposition of Zn-Graphite Oxide Nanocomposite Coatings on Stainless Steel from Sulfate Bath, its Surface Morphological and Corrosion Protection Studies. *Asian Journal of Chemistry*, 29(4), 917-922.
5. Geduld, H. (1988). *Zinc plating: Finishing Publications*.
6. *Standard Guide for Cleaning Metals Prior to Electroplating*. ASTM International, 2014.
7. Mandich, N.V. (2002). Surface Preparation of Metals Prior to Plating. *AESF SUR/FIN Proceedings*, 761-828.
8. Surhone, L.M., Timpledon, M.T. & Marseken, S.F. (2010). *Saponification* : Betascript Publishing.
9. Schramm, L.L., Stasiuk, E.N. & Marangoni, D.G. (2003). 2 Surfactants and their applications. *Annual Reports Section " C"(Physical Chemistry)*, 99, 3-48.
10. Yamashita, Y., Miyahara, R., & Sakamoto, K. (2017). *Emulsion and Emulsification Technology*. 489-506.
11. <https://asterionstc.com/2013/12/the-basics-of-alkaline-cleaning/>, (Accessed 22 April 2020).
12. Urréjola, S.R., Garcíaís, J.L. & Devesa-Rey, R. (2016). Optimization of Electrolytic Cleaning of Low Carbon Steels. *European Journal of Sustainable Development*, 5(3), 197-197. doi.org/10.14207/ejsd.2016.v5n3p197

13. Tang, B., Li, D., Fu, F., Xu, Y., Yu, G. & Zhang, J., (2012). A strategy for cleaner pickling: effect, mechanism, and evaluation method of a complex-inhibitor in hydrochloric acid medium. *Industrial & engineering chemistry research*, 51(6), 2615-2621.
14. Darken, J. (1979). Recent progress in bright plating from zincate electrolytes. *Transactions of the IMF*, 57(1), 145-151.
doi.org/10.1080/00202967.1979.11870505
15. Bockris, J.O.M. & Conway, B.E. (1994). *Modern Aspects of Electrochemistry: No. 26*. Springer Science & Business Media., 167-168.
16. Schlesinger, M. & Paunovic, M. (2014). *Modern Electroplating*. Hoboken, UNITED STATES: John Wiley & Sons, Incorporated., 423-452.
17. Dubpemell, G. (1978). *Met. Finish*, 76(1), 33.
18. Saubestre, E.B., Hajdu, J. & Zehnder, J. (1969). Acid zinc plating solutions for decorative applications. *Plating*, 56(6), 691-698.
19. Geduld, H. (1988). *Zincate or Alkaline non-cyanide Zinc Plating in 'Zinc Plating'*. ASM International Metals Park, Ohio, 90-110.
20. Loto, C.A. (2012). Electrodeposition of zinc from acid based solutions: a review and experimental study. *Asian Journal of Applied Sciences*, 5(6), 314-326.
21. Gamburg, Y.D. & Zangari, G. (2011). *Theory and Practice of Metal Electrodeposition*. Springer Science & Business Media, 284-289.
22. Tuaweri, T.J., Adigio, E.M. & Jombo, P.P. (2013). A study of process parameters for zinc electrodeposition from a sulphate bath. *International Journal of Engineering Science Invention*, 2(8), 17-24.
23. Li, M.C., Jiang, L.L., Zhang, W.Q., Qian, Y.H., Luo, S.Z. & Shen, J.N. (2007). Electrodeposition of nanocrystalline zinc from acidic sulfate solutions containing thiourea and benzalacetone as additives. *Journal of Solid State Electrochemistry*, 11(4), 549-553. doi.org/10.1007/s10008-006-0194-z
24. Meas, L.E.M.Y., Ortega-Borges, R., Perez-Bueno, J.J., Ruiz, H. & Trejo, G. (2009). Effect of a poly (ethylene glycol)(MW 200)/benzylideneacetone additive mixture on Zn electrodeposition in an acid chloride bath. *Int J Electrochem Sci*, 4, 1735-1753

25. Loto, C.A. (1992). Influence of Organic Additives on the Surface Characteristics of Zinc Electrodeposition on Mild Steel in Acid-Chloride solution: Ph, Bath-Composition and Time-variation Effects. *Corrosion Prevention and Control*, 142-149
26. Ito, K. & Sakakibara, T. (2011). *Acid zinc plating bath*. EP2357269A1.
27. Sato, A. (1994). *ASM Handbook, Zinc plating*. Surface Engineering, 5.
28. Herdman, R.D., Pearson, T. & Rowan, A., MacDermid Inc. (2006). *Zinc and zinc alloy electroplating additives and electroplating methods*. U.S. Patent 7, 109, 375.
29. Bai, A., Yang, K.L., Chen, H.L., Hong, Y.H. & Chang, S.B. (2017). High current density on electroplating smooth alkaline zinc coating. In *MATEC Web of Conferences* (Vol. 123, p. 00024). EDP Sciences. doi.org/10.1051/mateconf/201712300024
30. Peng, W.J. & Wang, Y.Y. (2007). Mechanism of zinc electroplating in alkaline zincate solution. *Journal of Central South University of Technology*, 14(1), 37-41. doi.org/10.1007/s11771-007-0008-1
31. Bockris, J.M., Nagy, Z. & Damjanovic, A. (1972). On the deposition and dissolution of zinc in alkaline solutions. *Journal of the electrochemical society*, 119(3), 285.
32. Wilcox, G.D. & Mitchell, P.J. (1987). The electrodeposition of zinc from zincate solutions. A review. *Transactions of the IMF*, 65(1), 76-79. doi.org/10.1080/00202967.1987.11870775
33. Schlesinger, M. & Paunovic, M. (2014). *Modern Electroplating*. Hoboken, UNITED STATES: John Wiley & Sons, Incorporated. 423-452.
34. Ortiz-Aparicio, J.L., Meas, Y., Trejo, G., Ortega, R., Chapman, T.W. & Chainet, E. (2013). Effects of organic additives on zinc electrodeposition from alkaline electrolytes. *Journal of Applied Electrochemistry*, 43(3), 289-300. doi.org/10.1007/s10800-012-0518-x
35. Oniciu, L. & Mureşan, L. (1991). Some fundamental aspects of levelling and brightening in metal electrodeposition. *Journal of applied electrochemistry*, 21(7), 565-574. doi.org/10.1007/BF01024843
36. Scott, M. & Moats, M. (2020). Optimizing Additive Ratios in Alkaline Zincate Electrodeposition. In *PbZn 2020: 9th International Symposium on Lead and Zinc Processing* (pp. 123-131). Springer, Cham. doi.org/10.1007/978-3-030-37070-1_11

37. Pushpavanam, M. (2006). Role of additives in bright zinc deposition from cyanide free alkaline baths. *Journal of applied electrochemistry*, 36(3), 315-322. <https://doi.org/10.1007/s10800-005-9076-9>
38. Acimovic, S., Lindermann, K.H., & Gunz, V.G. (1979). *Cyanide-free Alkaline Zinc Baths*. US. Pat. 4166778.
39. Ravindran, V., Krishnan, R.M. & Muralidharan, V.S. (1998). Characteristics of an alkaline tartrate zinc plating bath. *Metal finishing*, 96(10), 10-15
40. Roserberg, W.E. & Geduld, H.H. (1974). *Composition of Baths and Additives for Electrodeposition of Bright Zinc From Aqueous, Alkaline, Electroplating Baths*. US Pat. 3803008.
41. Onkarappa, N.K., Adarakatti, P.S. & Malingappa, P. (2017). A study on the effect of additive combination on improving anticorrosion property of zinc electrodeposit from acid chloride bath. *Industrial & Engineering Chemistry Research*, 56(18), 5284-5295. doi.org/10.1021/acs.iecr.7b00154
42. Liang, Y.U.A.N., Ding, Z.Y., Liu, S.J., Shu, W.F. & He, Y.N. (2017). Effects of additives on zinc electrodeposition from alkaline zincate solution. *Transactions of Nonferrous Metals Society of China*, 27(7), 1656-1664. doi.org/10.1016/S1003-6326(17)60188-2
43. Zuniga, V., Ortega, R., Meas, Y. & Trejo, G. (2004). Electrodeposition of Zinc from an Alkaline Non-cyanide Bath: Influence of a Quaternary Aliphatic Polyamine. *Plating and surface finishing*, 91(6), 46-51.
44. Naik, Y.A. & Venkatesha, T.V. (2005). A new condensation product for zinc plating from non-cyanide alkaline bath. *Bulletin of Materials Science*, 28(5), 495-501. doi.org/10.1007/BF02711243
45. Hsieh, J.C., Hu, C.C. & Lee, T.C. (2009). Effects of polyamines on the deposition behavior and morphology of zinc electroplated at high-current densities in alkaline cyanide-free baths. *Surface and Coatings Technology*, 203(20-21), 3111-3115. doi.org/10.1016/j.surfcoat.2009.03.035
46. Boto, K. (1975). Organic additives in zinc electroplating. *Electrodeposition and Surface Treatment*, 3(2), 77-95. doi.org/10.1016/0300-9416(75)90048-6
47. Kardos, O. (1974). Current distribution on microprofiles. *Plating*, 61(2), 129.
48. Watson, S.A. & Edwards, J. (1956). An investigation of the mechanism of levelling in electrodeposition. *Transactions of the IMF*, 34(1), 167-198. doi.org/10.1080/00202967.1956.11869725

49. Yang, X., Liu, S., Tang, J., Chang, G., Fu, Y., Jin, W., Ji, X. & Hu, J. (2019). Effective inhibition of zinc dendrites during electrodeposition using thiourea derivatives as additives. *Journal of Materials Science*, 54(4), 3536-3546. doi.org/10.1007/s10853-018-3069-7
50. Aaboubi, O., Douglade, J., Abenaqui, X., Boumedmed, R. & VonHoff, J. (2011). Influence of tartaric acid on zinc electrodeposition from sulphate bath. *Electrochimica acta*, 56(23), 7885-7889. doi.org/10.1016/j.electacta.2011.05.121
51. E.J., W. (1936). *Method of coating zinc or cadmium base metals*. p. US Patent 2035380.
52. Jelinek, T.W. (1982). *Galvanisches Verzinken (Eugen G. Leuze Verlag, Saulgau)*.
53. Wharton, J.A., Wilcox, G.D. & Baldwin, K.R. (1999). An electrochemical evaluation of possible non-chromate conversion coating treatments for electrodeposited zinc-nickel alloys. *Transactions of the IMF*, 77(4), 152-158. doi.org/10.1080/00202967.1999.11871272
54. Sonntag, B., *Cr (VI)-Free Post-Treatment Processes for Zinc & Zinc Alloys*.
55. Zouboulis, A.I., Prochaska, C.A. & Solozhenkin, P.M. (2005). Removal of zinc from dilute aqueous solutions by galvanochemical treatment. *Journal of Chemical Technology & Biotechnology: International Research in Process, Environmental & Clean Technology*, 80(5), 553-564. doi.org/10.1002/jctb.1233
56. Kobya, M., Demirbas, E., Ozyonar, F.U.A.T., Sirtbas, G. & Gengec, E.R.H.A.N. (2017). Treatments of alkaline non-cyanide, alkaline cyanide and acidic zinc electroplating wastewaters by electrocoagulation. *Process Safety and Environmental Protection*, 105, 373-385. doi.org/10.1016/j.psep.2016.11.020
57. https://www.ecfr.gov/cgi-bin/text-idx?SID=15e352a79a295dd3e0f1699119f82c04&mc=true&node=se40.31.401_115&rgn=div8, (Accesssed, 1/14/2022).
58. Agency, U.S.E.P. (1984). *Guidance manual for electroplating and metal finishing "ELECTROPLATING CATEGORICAL PRETREATMENT STANDARDS"*. 5.
59. Blais, J.F., Djedidi, Z., Cheikh, R.B., Tyagi, R.D. & Mercier, G. (2008). Metals precipitation from effluents. *Practice Periodical of Hazardous, Toxic, and Radioactive Waste Management*, 12(3), 135-149.
60. Nassef, E. & Eltaweel, Y. (2019). Removal of Zinc from aqueous solution using activated oil shale. *Journal of Chemistry*. doi.org/10.1155/2019/4261210

61. Eom, T.H., Lee, C.H., Kim, J.H. & Lee, C.H. (2005). Development of an ion exchange system for plating wastewater treatment. *Desalination*, 180(1-3), 163-172. doi.org/10.1016/j.desal.2004.11.088
62. Panda, R., Kumari, A., Hait, J. & Jha, M.K. (2016). Extraction and separation of zinc and chromium from electroplating effluent. *Journal of Metallurgy and Materials Science*, 58(4), 181-190.
63. Adhoum, N., Monser, L., Bellakhal, N. & Belgaied, J.E. (2004). Treatment of electroplating wastewater containing Cu^{2+} , Zn^{2+} and Cr (VI) by electrocoagulation. *Journal of hazardous materials*, 112(3), 207-213. doi.org/10.1016/j.jhazmat.2004.04.

VITA

Abdul Jalil Mohammed was born in Accra, Ghana. He earned his Bachelor of Science in Minerals Engineering from the University of Mines and Technology, Ghana, in 2017.

After obtaining his bachelor's degree, Abdul worked as a field extension officer at the Ministry of Food and Agriculture, Ghana. During this period, he trained and educated food processors on the effects of metallic contaminants from attrition mills used in grinding grains.

He earned his Master of Science in Metallurgical Engineering from the Missouri University of Science and Technology in May 2022 under the tutelage of Professor Michael Moats.